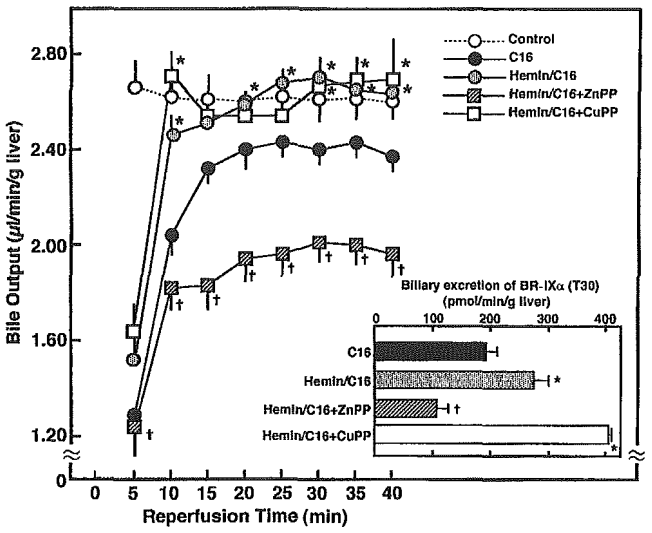

Fig. 2. Temporal alterations in the reperfusion-induced recovery of bile output in the 16-hour cold storage liver grafts *ex vivo*. ○ and ●, data collected from the control grafts and those undergoing 16-hour cold storage (C16), respectively; ● and ▨, data collected from grafts undergoing hemin treatment before cold storage and reperfusion (Hemin/C16) and those reperfused with 1 μmol/L ZnPP, an HO inhibitor (Hemin/C16 + ZnPP); □, data from the hemin-treated grafts undergoing reperfusion with 1 μmol/L CuPP (Hemin/C16 + CuPP). Data represent mean ± SE of 9-12 separate experiments. $*P < .05$ compared with the hemin-untreated liver grafts. $\dagger P < .05$ compared with the liver grafts undergoing HO-1 induction without ZnPP treatment. **(Inset)** Differences in the biliary flux of bilirubin (BR)-IXα among the 4 groups. Data were collected 30 minutes after the start of reperfusion. $*P < .05$ compared with the liver grafts without the hemin treatment; $\dagger P < .05$ compared with the hemin-treated grafts without the ZnPP treatment.

of bile output was greater than that observed between the C16 and hemin/C16 groups, suggesting that administration of ZnPP not only blocked the induced HO-1 activities but also suppressed constitutive activities of HO-2 in the grafts. Such a notion was supported by the data in the inset; the ZnPP-induced decrease in the bilirubin flux in hemin-treated C16 grafts was greater than the difference in the flux between hemin-treated and -untreated grafts.

The C16 grafts excreted bilirubin at approximately 200 pmol/min/g liver, which is comparable to the value measured in those undergoing the 30-minute control perfusion without cold storage.[28] When the grafts were pretreated with hemin and followed by 16-hour cold storage and 30-minute reperfusion, the bilirubin flux was significantly elevated (approximately 1.5-fold greater than that in the hemin-untreated group). However, this elevation was rather smaller than that of the venous CO increase in the same group (3-fold) (Fig. 1B). Such a stoichiometric discrepancy between the 2 heme-degrading products could result from decreased efficiency of bilirubin transport in the hemin-treated C16 grafts, as discussed later. The coperfusion of an HO inhibitor ZnPP, but not that of CuPP, completely attenuated and further suppressed bilirubin excretion, suggesting that the effects of ZnPP result from its ability to block HO activities (Fig. 2). These results led us to hypothesize that the catalytic activities of HO and actual heme degradation in the graft determine the recovery of bile output in the post–cold ischemic liver grafts.

Bilirubin Accounts for a Crucial Player for the HO-1–Mediated Protection of the Grafts. In the next series of experiments, we examined whether supplementation of the reaction product(s) of HO could alter the hepatobiliary parameters of the grafts. The plasma bilirubin concentrations in portal blood samples collected from the hemin-treated rats were 3.2 ± 0.8 μmol/L (n = 4), whereas those in the control were less than 1.0 μmol/L.[29] Based on these data, physiologically relevant concentrations of bilirubin in the hemin-treated livers could be estimated to be approximately 5 μmol/L. Figure 3A to C shows the effects of supplementation of bilirubin and/or CO at 5 μmol/L on the ZnPP-induced repression of bile output, biliary excretion of bile salts, and phospholipids in the 16-hour cold-stored grafts. As seen, hemin pretreatment markedly improved these bile excretory parameters. HO blockade by ZnPP cancelled these effects of hemin pretreatment. The improvement of biliary indices by hemin was restored by supplementation of bilirubin even in the presence of ZnPP. Such beneficial effects of bilirubin were not substituted by supplementation of CO at the same concentration. Furthermore, supplementation of both of these products did not enhance the beneficial effects of bilirubin by itself.

We further examined dose-dependent effects of supplementation of bilirubin and CO (Fig. 4A-C). Effects of bilirubin on biliary function were obviously biphasic; bile output and biliary fluxes of bile salts and phospholipids exhibited a marked recovery at concentrations in a range between 1 and 5 μmol/L and showed a significant reduction at concentrations greater than 5 μmol/L. On the other hand, supplementation of CO did not cause any notable recovery of these indices, suggesting that bilirubin rather than CO contributes to improvement of biliary function in the HO-1–preconditioned liver grafts. The impairment of biliary function by C16 treatment and its recovery by HO-1 induction seem to occur in parallel with alterations in cell viability. As shown in Fig. 5, C16 treatment significantly increased venous LDH release. Hemin pretreatment suppressed enzyme release almost completely. Because administration of ZnPP significantly increased enzyme release, the loss of cell viability seemed to depend on the HO activities. The cancellation of the improving effect of HO-1 by ZnPP was restored in a dose-dependent manner by exogenous supplementation

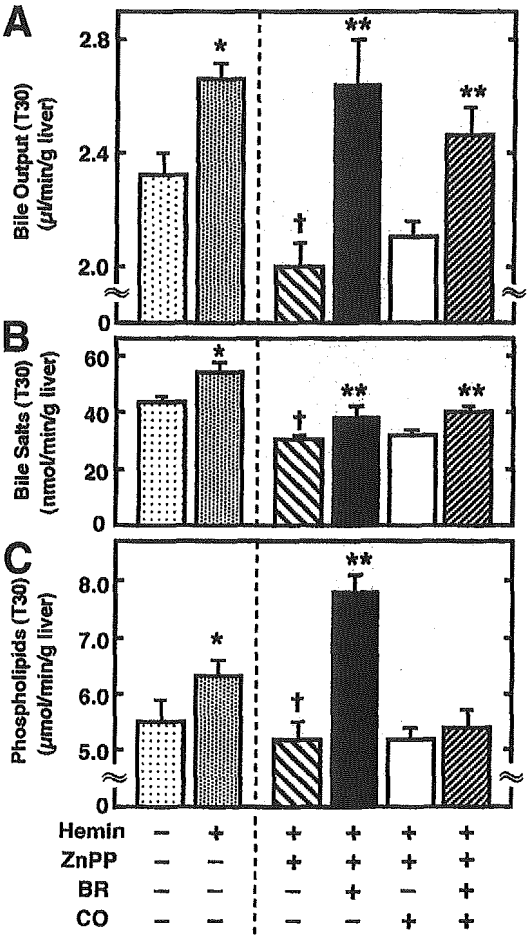

Fig. 3. Suppression of the HO-1-elicited improvement of bile formation by ZnPP and restoration effects of supplementation with bilirubin and/or CO in the cold storage grafts reperfused *ex vivo*. Restoration effects of bilirubin and/or CO at 5 μmol/L on the ZnPP-induced suppression of (A) bile output, (B) biliary fluxes of bile constituents such as bile salts, and (C) phospholipids in the hemin-pretreated grafts. Data were collected 30 minutes after the onset of reperfusion. $*P < .05$ compared with the grafts undergoing 16-hour cold storage (C16); $\dagger P < .05$ compared with the hemin-pretreated grafts undergoing C16; $**P < .05$ compared with the hemin-pretreated grafts perfused with 1 μmol/L ZnPP. Note that bilirubin at 5 μmol/L exhibited significant restoration effects, whereas CO at the same concentration did not cause such effects. Data indicate mean ± SE of 9-12 separate experiments.

of bilirubin at no greater than 5 μmol/L, while its supplementation at 10 μmol/L was cytotoxic. These results suggest that bilirubin plays a pivotal role in mechanisms for the HO-1–mediated protection of the post–cold ischemic liver grafts.

***Short-term Bilirubin Supplementation Attenuates the Reperfusion Injury* Ex Vivo.** Current observations suggesting that bilirubin accounts for the mechanism for HO-1–mediated protection led us to inquire whether a simple supplementation of this bile pigment could substitute for the hepatoprotective effects of the HO-1 preconditioning against CI/R injury *ex vivo*. Because high doses of bilirubin were shown to be cytotoxic, we chose 5 μmol/L bilirubin to be tested and carefully designed perfusion protocols (Fig. 6). The first group was treated with the 5-minute perfusion with the buffer containing 5 μmol/L bilirubin (plot a), whereas the second and third groups were treated with the 15-minute and 40-minute perfusion with the same concentration of bilirubin (plots b and c), respectively. As seen in Fig. 6A, the C16 grafts undergoing the 5-minute bilirubin supplementation significantly improved bile output compared with the control (closed circles vs. open circles). When the intervals for bilirubin supplementation were extended to 15 and 40 minutes (plots b and c), bile output was significantly reduced compared with the control and the 5-minute perfusion groups (Fig. 6B). Such dose-dependent effects of bilirubin

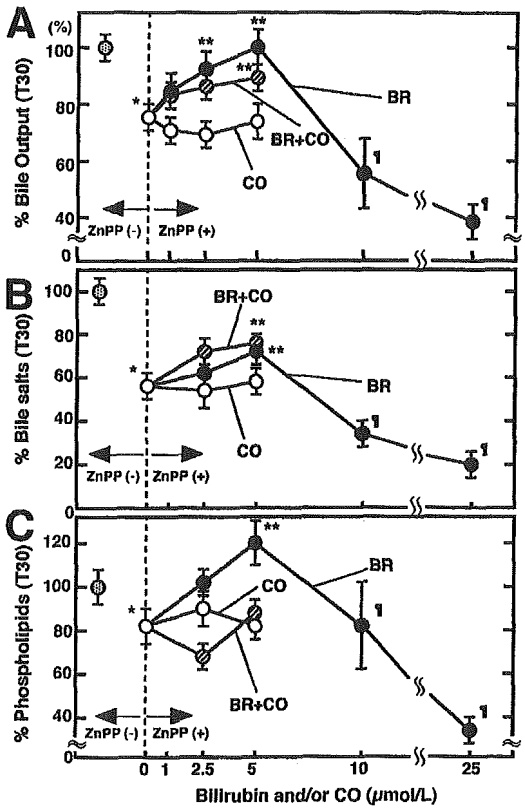

Fig. 4. Dose-dependent restoration effects of exogenous supplementation with bilirubin (BR) and/or CO on the ZnPP-induced impairment of biliary function in the hemin-pretreated grafts reperfused *ex vivo*. Alterations in relative changes in (A) bile output, (B) biliary fluxes of bile salts, and (C) phospholipids as a function of concentrations of exogenously administered BR and/or CO. The values of these parameters of the grafts were expressed as percentages versus the corresponding values determined in the hemin-pretreated 16-hour cold storage grafts (● near y-axes). Data were collected 30 minutes after the onset of reperfusion. ●, ○, and ▨ denote data from the grafts treated with BR, CO, and both, respectively. $*P < .05$ compared with data from the cold storage grafts undergoing HO-1 preconditioning; $**P < .05$ compared with the HO-1-inducing grafts treated with 1 μmol/L ZnPP but without BR or CO; $\P P < .05$ compared with the grafts treated with 5 μmol/L BR. Note that BR at less than 5 μmol/L exhibited significant restoration effects, whereas that at greater concentrations caused a marked reduction of bile formation. Data indicate mean ± SE of 6-12 separate experiments.

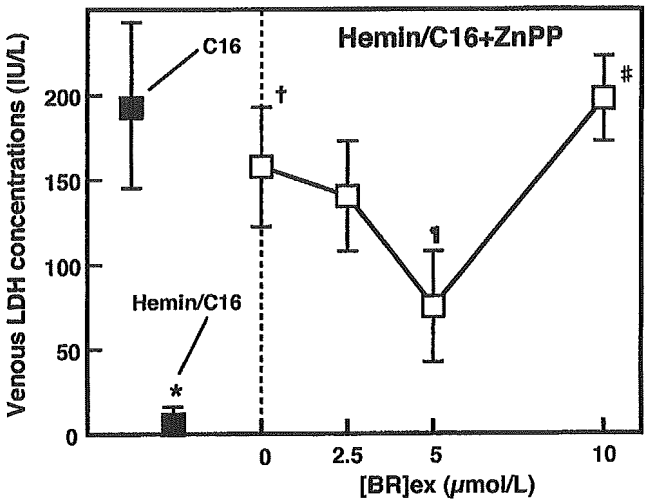

Fig. 5. Effects of exogenously applied bilirubin ([BR]ex) on the ZnPP-elicited aggravation of cell injury in the hemin-treated 16-hour cold storage grafts reperfused *ex vivo*. *$P < .05$ compared with the C16-treated grafts; †$P < .05$ compared with the hemin/C16-treated livers; ¶$P < .05$ compared with the hemin-pretreated grafts treated with 1 μmol/L ZnPP; #$P < .05$ compared with the grafts treated with 5 μmol/L bilirubin. Data indicate mean ± SE of 5-6 separate livers.

on bile output coincided with alterations in venous LDH release from the grafts. The 5-minute bilirubin treatment significantly attenuated the C16-induced elevation of LDH, whereas the longer periods of the supplementation aggravated the release of the enzyme. As shown previously in Figs. 3 to 5, the 30-minute coperfusion of 5 μmol/L bilirubin in the presence of ZnPP did not cause any harmful effects on bile excretion and cell viability in the hemin-pretreated C16 grafts, implicating different sensitivity to exogenous bilirubin between the hemin-treated and -untreated grafts. Considering the observation showing a discrepancy between the venous CO flux and biliary bilirubin excretion in the hemin-treated grafts (Figs. 1 and 2), these results suggest that pharmacologic interventions to induce HO-1 in the graft could alter physiologic processes of entry and excretion of bilirubin.

Figure 7 summarizes differences in cell injury among groups as judged by the release of aspartate aminotransferase and LDH into the venous perfusate 30 minutes after the start of reperfusion *ex vivo*. As shown, the release of both enzymes was significantly elevated in the C16-treated grafts compared with that in the normoperfused livers. Hemin pretreatment for the HO-1 preconditioning significantly suppressed enzyme release, which was cancelled by blocking HO with ZnPP. On the other hand, the short-term coperfusion of bilirubin (C16 + BR) attenuated the C16-induced elevation of the enzyme release downward to the level comparable to that in the hemin-treated grafts, mimicking protective effects of the HO-1 preconditioning against CI/R injury.

***Protective Effects of Bilirubin Rinse Against Post-transplant Cholestasis and Injury* In Vivo.** *Ex vivo* results showing beneficial effects of short-term rinse treatment with bilirubin encouraged us to reproduce such hepatoprotective effects of bilirubin rinse on posttransplant injury *in vivo*. As seen in Fig. 8A, pretransplant rinse of the grafts with bilirubin (closed circles) altered bile output both in the early (onset) and late (24-hour) phases of reperfusion in a biphasic manner. The rinse with bilirubin at 5 to 10 μmol/L significantly improved bile output, whereas that at greater concentrations caused cholestasis by contrast. No rats receiving grafts rinsed with bilirubin at 50 μmol/L were able to survive for 24 hours after transplantation. Similarly, the bilirubin rinse dose-dependently altered cell injury as judged by the release of enzymes (serum aspartate aminotransferase, serum alanine aminotransferase, and serum LDH). As shown in Fig. 8B, the rinse at 5 to 10 μmol/L reduced the cell injury, whereas that at greater concentrations aggravated it. It should be noted that the graft rinse with 5 to 10 μmol/L bilirubin attenuated postreperfusion cholestasis and cell injury *in vivo* downward to the level comparable to those in the grafts undergoing the HO-1 precondition-

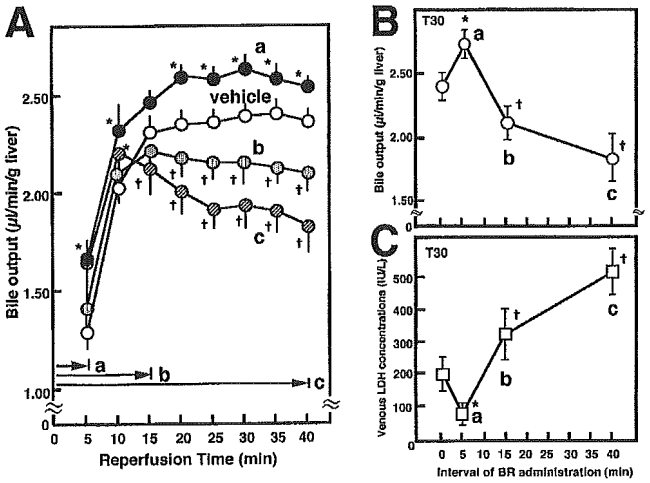

Fig. 6. Effects of different durations of *ex vivo* coperfusion of bilirubin on bile output and cell injury in the hemin-untreated liver grafts undergoing 16-hour cold storage (C16). (A) Different temporal patterns of the reperfusion-induced recovery of bile output with varied durations of the bilirubin reperfusion. ○, data from the C16-treated grafts perfused without bilirubin. ●, ◍, and ◍ indicate those from the grafts reperfused with 5 μmol/L bilirubin for (a) 5 minutes, (b) 15 minutes, and (c) 40 minutes, respectively. *$P < .05$; significantly greater than the C16-treated grafts. †$P < .05$; significantly less than the C16-treated grafts. Note that the 5-minute bilirubin supplementation significantly improves the recovery of bile output. (B and C) Alterations in the recovery of bile output measured at 30 minutes (T30) and the venous LDH release as a function of the intervals of the bilirubin supplementation. The concentration of bilirubin applied was 5 μmol/L in B and C. *$P < .05$; significantly (B) greater and (C) less than the C16-treated grafts. †$P < .05$; significantly (B) less than and (C) greater than the C16-treated grafts. Data indicate mean ± SE of 5-6 separate grafts.

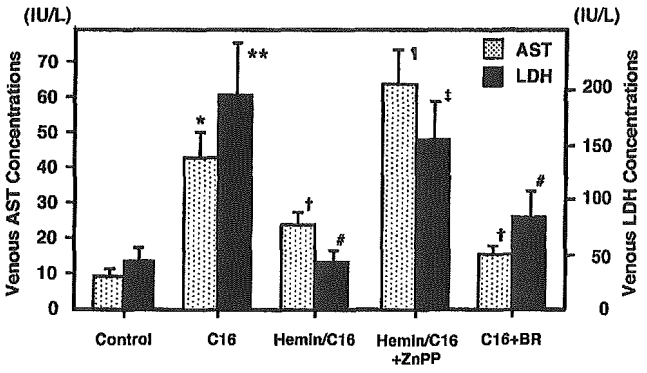

Fig. 7. Amelioration of cell injury by bilirubin rinse or HO-1 preconditioning in 16-hour cold ischemic grafts undergoing 30-minute reperfusion. ■ and ■ denote contents of aspartate aminotransferase (AST) and LDH released in the venous perfusate 30 minutes after the start of reperfusion *ex vivo*, respectively. Control, normoperfused livers without cold ischemia; C16, 16-hour cold storage grafts; hemin/C16, hemin-pretreated grafts undergoing 16-hour cold storage; hemin/C16 + ZnPP, hemin/C16-treated grafts undergoing coperfusion of ZnPP; C16 + BR, C16-treated grafts undergoing 5-minute rinse with 5 μmol/L bilirubin on reperfusion. $*P < .05$, $**P < .05$; significantly greater than controls. $\dagger P < .05$, $\#P < .05$; significantly less than the C16-treated grafts. $\P P < .05$, $\ddagger P < .05$; significantly greater than the hemin/C16-treated grafts. Data represent mean ± SE of 4-6 separate grafts.

ing with hemin (Fig. 8, hemin [+]). These results not only clarified *in vivo* protective effects of the HO-1 preconditioning against hepatic CI/R injury but also suggested that this procedure could be substituted by the rinse with low-dose bilirubin.

Improved Survival of the Grafts Rinsed With Low-Dose Bilirubin. Posttransplant 24-hour survival of rats undergoing the graft rinse with lactated Ringer's solution alone was 67%; the ratio of the number of surviving versus transplanted rats was 8/12. The graft rinse with 5 μmol/L bilirubin did not alter the survival significantly (the ratio was 8/11), whereas rats receiving grafts rinsed with 10 or 20 μmol/L bilirubin significantly improved the survival rate (100% [10/10] or 100% [10/10], respectively). By contrast, when the grafts were rinsed with 50 μmol/L bilirubin, the survival rate became zero (0/6), which is significantly lower than the rate in the group without bilirubin rinse. On the other hand, the survival rate of rats transplanted with hemin-pretreated grafts was 100% (10/10), which is significantly greater than that of those receiving grafts rinsed with lactated Ringer's solution alone. These results suggest that pretransplant rinse with bilirubin at optimal concentrations improved survival of 16-hour preserved grafts, whereas the greater dose of this reagent decreased survival rates.

Parenchymal Delivery of Bilirubin to Attenuate Oxidative Stress of the Grafts. Figure 9A to C shows immunohistochemical analyses showing effects of the bilirubin rinse on delivery of the bile pigment into the graft tissues. As seen in the graft rinsed with lactated Ringer's solution, immunoreactivities of anti–bilirubin-IXα monoclonal antibody 24G7 occurred mainly in nonparenchymal cells including Kupffer cells, a major cellular component of the HO-1 expression,[21] and were also detectable faintly in the parenchymal regions compared with its negative control. When the graft was rinsed with bilirubin, the reagent was taken up into parenchymal cells and caused a notable elevation of the immunoreactivities. These results suggest that the present rinse procedure can effectively transfer bilirubin into hepatocytes of the grafts.

We further investigated if the bilirubin rinse could attenuate reperfusion-induced oxidative changes in the grafts. As judged by immunoreactivities of anti-acrolein monoclonal antibody 5F6 (Fig. 10), the grafts undergoing the 16-hour cold storage showed notable oxidative stress in nuclei of hepatocytes (Fig. 10B vs. 10A). These changes were attenuated by the hemin pretreatment (Fig. 10C) or by the bilirubin rinse (Fig. 10D). Morphometric analyses showed that the average number of hepatocytes

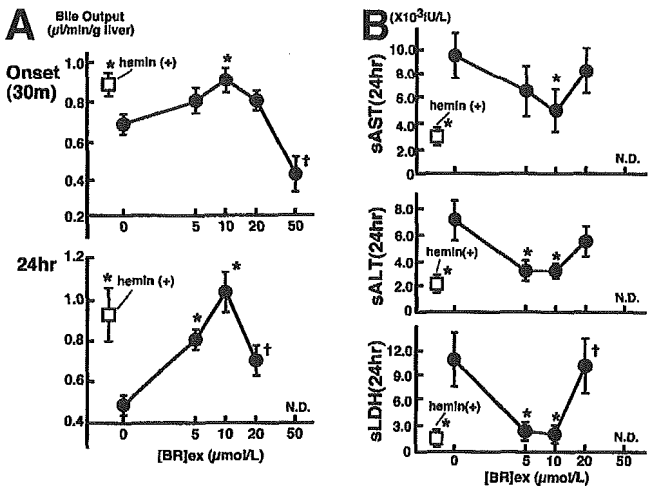

Fig. 8. *In vivo* protective effects of bilirubin rinse against posttransplant cholestasis and cell injury in the liver grafts undergoing 16-hour cold storage. □, data showing beneficial effects of the HO-1 induction by hemin; ●, data collected from grafts rinsed with varied concentrations of free bilirubin and reperfused *in vivo*. (A) Alterations in bile output *in vivo* at the onset of reperfusion (30 minutes, top) and 24 hours (bottom) after reperfusion as a function of concentrations of bilirubin administered as a pretransplant rinse agent ([BR]ex). N.D., no rats receiving grafts rinsed with lactated Ringer's solution containing 50 μmol/L bilirubin were able to survive for 24 hours. (B) Alterations in the graft injury *in vivo* as judged by the release of enzymes (serum aspartate aminotransferase [AST], serum alanine aminotransferase [sALT], and serum LDH [sLDH]) by the bilirubin rinse. Data were collected 24 hours after revascularization. Note that the graft rinse with 5-10 μmol/L bilirubin reduced cell injury downward to a level comparable to that in the HO-1-preconditioned grafts, whereas its greater concentrations enhanced the injury by contrast. $*P < .05$ compared with the grafts rinsed with lactated Ringer's solution without bilirubin; $\dagger P < .05$ compared with the grafts rinsed with lactated Ringer's solution containing 10 μmol/L bilirubin. Data indicate mean ± SE of 5-8 separate grafts.

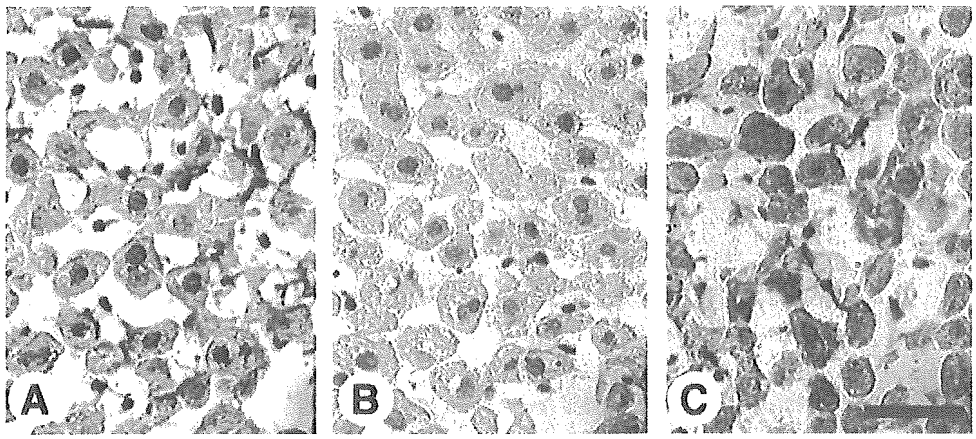

Fig. 9. Distribution of bilirubin in the grafts treated with the bilirubin rinse shown by the anti-bilirubin IXα monoclonal antibody 24G7. (A) The graft rinsed with lactated Ringer's solution without bilirubin. Note the presence of bilirubin in nonparenchymal cells and also faintly in hepatocytes. (B) A negative control image in the absence of the primary monoclonal antibody 24G7. (C) The graft treated with the bilirubin rinse. Nuclear staining by methyl green was performed in all micrographs. **Bar** = 50 μm.

with acrolein-positive nuclei in the 16-hour cold-stored grafts was 2,398 ± 137/mm^2 (n = 3), which was significantly greater than that in control (0 ± 0/mm^2, n = 3). The number in the cold-stored grafts with hemin pretreatment or bilirubin rinse was 1,603 ± 171/mm^2 (n = 3) or 815 ± 207/mm^2 (n = 3), respectively, which was significantly smaller than the number in the 16-hour stored grafts without these treatments. These results suggest that the HO-1 preconditioning as well as the bilirubin rinse significantly reduced oxidative stress.

Discussion

The current study provides evidence that preconditioning of the liver graft with the HO-1 induction ameliorated CI/R-induced hepatobiliary dysfunction *ex vivo*

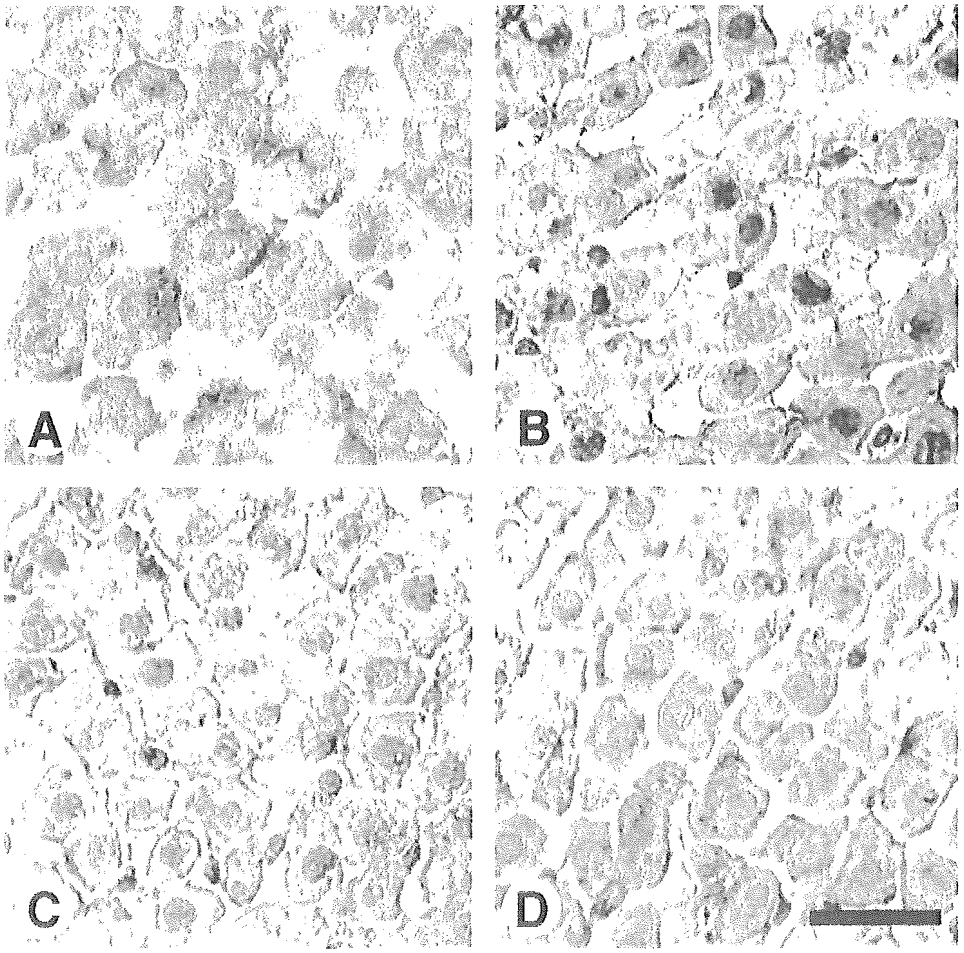

Fig. 10. Representative pictures showing immunoreactivities of protein-bound acrolein in the reperfused liver grafts. All samples were fixed at 30 minutes after the start of reperfusion *ex vivo*. (A) Control liver without any treatment. (B) The 16-hour cold ischemic grafts. (C) The 16-hour cold storage grafts undergoing HO-1 preconditioning with hemin treatment. (D) The cold-stored grafts undergoing the 5-minute rinse with 5 μmol/L bilirubin on reperfusion. **Bar** = 25 μm.

and *in vivo* and that the protection mechanisms involve actions of bilirubin. Several lines of evidence supported this concept. First, the HO-1 preconditioning coincided with overproduction of bilirubin in the liver grafts even after reperfusion. Second, exogenous supplementation of low-dose bilirubin rather than CO reproduced the beneficial effects of the preconditioning even under inhibition of HO-1 on reperfusion. Third, the preconditioning significantly reduced oxidative stress in parenchyma, improving biliary dysfunction and hepatocellular injury. Finally, the bilirubin rinse by itself reduced hepatocellular oxidative damage and graft dysfunction to the level comparable to that with the HO-1 preconditioning. Considering important roles of oxidative stress in the 16-hour CI/R injury,[6] these results first provided evidence *ex vivo* and *in vivo* for crucial roles of this antioxidant bile pigment in graft protection.

The most important result in the current study is the fact that a simple supplementation of bilirubin at the early phase of reperfusion could substitute for the HO-1 preconditioning effects. As shown in Figs. 6 and 7, the short-term bilirubin rinse turned out to exert significant protective actions on postreperfusion graft viability *ex vivo*. By contrast, long-term supplementation of bilirubin seemed to be harmful because of the intrahepatic accumulation of the substance, causing cytotoxic effects on the graft. Protective effects of the rinse treatment with low-dose bilirubin were reproduced in experiments *in vivo*, improving the posttransplant graft viability and survival. Therefore, an initial flush of the cold-stored liver on reperfusion by exogenous bilirubin at the optimal concentrations could serve as a potentially promising stratagem for ameliorating CI/R injury.

Our data collected from perfused grafts were obviously inconsistent with previous results showing beneficial effects of CO supplementation against the reperfusion-induced graft injury *ex vivo*.[30] According to that previous study, exogenously applied CO could regulate mitogen-activated proliferation kinase and thereby improve the graft viability. Careful comparison of experimental protocols between our study and that study showed that the presence or absence of erythrocytes in the perfusate could influence effects of the CO supplementation on the *ex vivo* reperfusion injury of the grafts. Distinct from our *ex vivo* study, the previous data were collected from the grafts reperfused with the erythrocyte-containing buffer. Under these circumstances, CO increases the affinity of molecular oxygen to hemoglobin and thereby interferes with oxygen delivery to the graft parenchyma. Such an effect of the gas could ameliorate the oxidative injury processes through a reduction of the delivery of molecular oxygen as a substrate for reactive oxygen species.[31,32] Our observation showing that CO did not exhibit any beneficial effects on the viability of hemoglobin-free perfused grafts *ex vivo* fully supports a concept that its protective action depends on effects of hemoglobin. Further investigation should thus be necessary to address if this gaseous monoxide could actually improve the posttransplant graft viability *in vivo*.

In the current study, the hemin-pretreated grafts undergoing CI/R exhibited a marked retardation of uptake and excretion of bilirubin, as indicated by their lesser susceptibility to long-term bilirubin perfusion as well as by notable discrepancy between the venous CO and biliary bilirubin fluxes. We previously reported that hemin treatment by the identical procedure *per se* induced stoichiometric elevation of the venous CO and biliary bilirubin fluxes in non–cold ischemic normoperfused livers.[19] Thus, the hemin treatment by itself did not retard the bilirubin uptake to parenchyma, but its combination with the CI/R could cause such a discrepancy in metabolism of the 2 heme-degrading products. Although the detailed molecular mechanisms for this event remain unknown, these data raised an important question as to which preconditioning intervention benefits a quality of the transplantation: pharmacologic HO-1 induction or the bilirubin rinse. As reported previously, hemin pretreatment is known to induce ferritin that captures ferrous iron and to up-regulate thioredoxin to ameliorate oxidative stress[33-35]; these pathways could serve as additive protective mechanisms besides those dependent on HO products against post–cold ischemic graft injury. However, this preconditioning reagent *per se* accounts for a catalyst of Fenton reaction and the resultant HO-1 induction could be harmful to the graft viability when amounts of ferrous iron released from the reaction are excessive.[36,37] In this context, short-term administration of bilirubin did not show any retarding effect on the endogenous bilirubin metabolism, as long as its concentrations are optimally kept. Considering clinical application of optimal procedures to protect liver grafts, the absence of interference with endogenous heme catabolism and the simplicity of costless procedures could be of greater advantage for the bilirubin rinse than the pharmacologic induction of HO-1 by hemin.

Acknowledgment: The authors thank Tokyo Electric Power Company Hospital and Hitomi Irisawa for supporting measurements of bile constituents.

References

1. Clavien PA, Harvey PRC, Strasberg SM. Preservation and reperfusion injuries in liver allografts: an overview and synthesis of current studies. Transplantation 1992;53:957-978.

2. Lemasters JJ, Bunzendahl H, Thurman RG. Reperfusion injury to donor livers stored for transplantation. Liver Transplant Surg 1995;1:124-138.
3. Greig PD, Woolf GM, Sinclair SB, Abecassis M, Strasberg SM, Taylor BR, Levy GA, et al. Treatment of primary liver graft nonfunction with prostaglandin E1. Transplantation 1989;48:447-453.
4. Caldwell-Kenkel JC, Currin RT, Tanaka Y, Thurman RG, Lemasters JJ. Kupffer cell activation and endothelial cell damage after storage of rat livers: effects of reperfusion. HEPATOLOGY 1991;13:83-95.
5. Gao W, Bentley RC, Madden JF, Clavien PA. Apoptosis of sinusoidal endothelial cells is a critical mechanism of preservation injury in rat liver transplantation. HEPATOLOGY 1998;27:1652-1660.
6. Kumamoto Y, Suematsu M, Shimazu M, Kato Y, Sano T, Makino N, Kitajima M, et al. Kupffer cell-independent acute hepatocellular oxidative stress and decreased bile formation in post-cold-ischemic rat liver. HEPATOLOGY 1999;30:1454-1463.
7. Nakamura T, Arii S, Monden K, Sasaoki T, Adachi Y, Ishiguro S, Imamura M, et al. Amelioration by Kupffer cell blockade in hepatic damage induced by cold preservation with subsequent plasma-supplemented perfusion. J Surg Res 1996;62:207-215.
8. Kukan M, Vajdova K, Horecky J, Nagyova A, Mehendale HM, Trnovec T. Effects of blockade of Kupffer cells by gadolinium chloride on hepatobiliary function in cold ischemia-reperfusion injury of rat liver. HEPATOLOGY 1997;26:1250-1257.
9. Takahashi Y, Tamaki T, Tanaka M, Konoeda Y, Kawamura A, Katori M, Kakita A. Efficacy of heat-shock proteins induced by severe fasting to protect rat livers preserved for 72 hours from cold ischemia/reperfusion injury. Transplant Proc 1998;30:3700-3702.
10. Matsumoto K, Honda K, Kobayashi N. Protective effect of heat preconditioning of rat liver graft resulting in improved transplant survival. Transplantation 2001;71:862-868.
11. Yin DP, Sankary HN, Chong ASF, Ma LL, Shen J, Foster P, Williams JW. Protective effect of ischemic preconditioning on liver preservation-reperfusion injury in rats. Transplantation 1998;66:152-157.
12. Amersi F, Buelow R, Kato H, Ke B, Coito AJ, Busuttil RW, Kupiec-Weglinski JW, et al. Upregulation of heme oxygenase-1 protects genetically fat Zucker rat livers from ischemia/reperfusion injury. J Clin Invest 1999;104:1631-1639.
13. Soares MP, Lin Y, Anrather J, Csizmadia E, Choi AM, Poss KD, Bach FH, et al. Expression of heme oxygenase-1 can determine cardiac xenograft survival. Nat Med 1998;4:1073-1077.
14. Maines MD. Heme oxygenase: function, multiplicity, regulatory mechanisms, and clinical applications. FASEB J 1988;2:2557-2568.
15. Kyokane T, Norimizu S, Taniai H, Naito M, Takeoka S, Tsuchida E, Nimura Y, et al. Carbon monoxide from heme catabolism protects against hepatobiliary dysfunction in endotoxin-treated rat liver. Gastroenterology 2001;120:1227-1240.
16. Ponka P, Beaumont C, Richardson DR. Function and regulation of transferrin and ferritin. Semin Hematol 1998;35:35-54.
17. Suematsu M, Goda N, Sano T, Kashiwagi S, Egawa T, Shinoda Y, Ishimura Y. Carbon monoxide: an endogenous modulator of sinusoidal tone in the perfused rat liver. J Clin Invest 1995;96:2431-2437.
18. Stocker R, Yamamoto Y, McDonagh AF, Glazer AN, Ames BN. Bilirubin is an antioxidant of possible physiological importance. Science 1987;235:1043-1046.
19. Wakabayashi Y, Takamiya R, Mizuki A, Kyokane T, Goda N, Suematsu M, Ishimura Y, et al. Carbon monoxide overproduced by heme oxygenase-1 causes a reduction of vascular resistance in perfused rat liver. Am J Physiol 1999;277:G1088-G1096.
20. Sano T, Shiomi M, Wakabayashi Y, Shinoda Y, Goda N, Yamaguchi T, Suematsu M, et al. Endogenous carbon monoxide suppression stimulates bile acid-dependent biliary transport in perfused rat liver. Am J Physiol 1997;272:G1268-G1275.
21. Goda N, Suzuki K, Naito M, Takeoka S, Tsuchida E, Ishimura Y, Suematsu M, et al. Distribution of heme oxygenase isoforms in rat liver: topographic basis for carbon monoxide-mediated microvascular relaxation. J Clin Invest 1998;101:604-612.
22. Shimizu S, Izumi Y, Yamazaki M, Shimizu K, Yamaguchi T, Nakajima H. Anti-bilirubin monoclonal antibody I. Preparation and properties of monoclonal antibodies to covalently coupled bilirubin-albumin. Biochim Biophys Acta 1988;967:255-260.
23. Izumi Y, Yamazaki M, Shimizu S, Shimizu K, Yamaguchi T, Nakajima H. Anti-bilirubin monoclonal antibody II. Enzyme-linked immunosorbent assay for bilirubin fractions by combination of two monoclonal antibodies. Biochim Biophys Acta 1988;967:261-266.
24. Tanaka A, Katagiri K, Hoshino M, Hayakawa T, Tsukada K, Takeuchi T. Endothelin-1 stimulates bile acid secretion and vesicular transport in the isolated rat liver. Am J Physiol 1994;266:G324-G329.
25. Uchida K, Kanematsu M, Sakai K, Matsuda T, Hattori N, Mizuno Y, Suzuki D, et al. Protein-bound acrolein: potential markers for oxidative stress. Proc Natl Acad Sci U S A 1998;95:4882-4887.
26. Kamada N, Calne RY. Orthotopic liver transplantation in the rat. Technique using cuff for portal vein anastomosis and biliary drainage. Transplantation 1979;28:47-50.
27. Ozawa N, Goda N, Makino N, Yamaguchi T, Yoshimura Y, Suematsu M. Leydig cell-derived heme oxygenase-1 regulates apoptosis of premeiotic germ cells in response to stress. J Clin Invest 2002;109:457-467.
28. Yamaguchi T, Wakabayashi Y, Tanaka M, Sano T, Ishikawa H, Suematsu M, Ishimura Y, et al. Taurocholate induces directional excretion of bilirubin into bile in perfused rat liver. Am J Physiol 1996;270:G1028-G1032.
29. Hayashi S, Takamiya R, Yamaguchi T, Matsumoto K, Makino N, Ishimura Y, Suematsu M, et al. Induction of heme oxygenase-1 suppresses venular leukocyte adhesion elicited by oxidative stress: role of bilirubin generated by the enzyme. Circ Res 1999;85:663-671.
30. Amersi F, Shen XD, Anselmo D, Melineck J, Busuttil RW, Buelow R, Kupiec-Weglinski JW, et al. *Ex vivo* exposure to carbon monoxide prevents hepatic ischemia/reperfusion injury through p38 MAP kinase pathway. HEPATOLOGY 2002;35:815-823.
31. Granger DN. Role of xanthine oxidase and granulocytes in ischemia-reperfusion injury. Am J Physiol 1988;255:H1269-H1275.
32. Jones DP. The role of oxygen concentration in oxidative stress: hypoxic and hyperoxic models. In: Sies H, ed. Oxidative Stress. New York: Academic, 1985:152-195.
33. Balla G, Jacob HS, Balla J, Rosenberg M, Nath K, Apple F, Eaton JW, et al. Ferritin: a cytoprotective antioxidant stratagem of endothelium. J Biol Chem 1992;267:18148-18153.
34. Kim YC, Matsutani H, Yamaguchi Y, Itoh K, Yamamoto M, Yodoi J. Hemin-induced activation of the thioredoxin gene by Nrf2. J Biol Chem 2001;276:18399-18406.
35. Mitsui A, Hirakawa T, Yodoi J. Reactive oxygen-reducing and protein-refolding activities of adult T cell leukemia-derived factor/human thioredoxin. Biochem Biophys Res Commun 1992;186:1220-1226.
36. Hori R, Kashiba M, Toma T, Yachie A, Goda N, Makino N, Suematsu M, et al. Gene transfection of H25A mutant heme oxygenase-1 protects cells against hydroperoxide-induced cytotoxicity. J Biol Chem 2002;277:10712-10718.
37. Bauer M, Bauer I. Heme oxygenase-1: redox regulation and role in the hepatic response to oxidative stress. Antioxid Redox Signal 2002;4:749-758.

THE JOURNAL OF BIOLOGICAL CHEMISTRY
Vol. 278, No. 23, Issue of June 6, pp. 21204–21211, 2003
Printed in U.S.A.

Identification of Outer Mitochondrial Membrane Cytochrome b_5 as a Modulator for Androgen Synthesis in Leydig Cells*

Received for publication, February 18, 2003, and in revised form, March 28, 2003
Published, JBC Papers in Press, March 31, 2003, DOI 10.1074/jbc.M301698200

Tadashi Ogishima‡, Jun-ya Kinoshita, Fumiko Mitani§, Makoto Suematsu§, and Akio Ito

From the Department of Chemistry, Faculty of Sciences, Kyushu University, Fukuoka 812-8581, Japan and the §Department of Biochemistry and Integrative Medical Biology, Keio University, Tokyo 160-8582, Japan

Outer mitochondrial membrane cytochrome b_5 is an isoform of microsomal membrane cytochrome b_5. In rat testes the outer mitochondrial membrane cytochrome b_5 is present in both mitochondria and microsomes, whereas microsomal membrane cytochrome b_5 is undetectable. Outer mitochondrial membrane cytochrome b_5 present in the testis was localized in Leydig cells with cytochrome P-450$_{17\alpha}$, which catalyzes androgenesis therein. We therefore analyzed the functions of outer mitochondrial membrane cytochrome b_5 in rat testis microsomes by using a proteoliposome system. In a low but physiological concentration of NADPH-cytochrome P-450 reductase and excess amount of progesterone, outer mitochondrial membrane cytochrome b_5 stimulated the cytochrome P-450$_{17\alpha}$-catalyzed reactions, 17α-hydroxylation and C17-C20 bond cleavage. The effects were different from those by microsomal membrane cytochrome b_5 as follows: preferential elevation of the 17α-hydroxylase activity by outer mitochondrial membrane cytochrome b_5 in an amount-dependent manner *versus* that of the lyase activity by microsomal membrane cytochrome b_5 at the low concentration, and the inhibition of both activities at the high concentration. At a low concentration of progesterone reflecting a physiological cholesterol supply, outer mitochondrial membrane cytochrome b_5 elevated primarily the production of 17α-hydroxyprogesterone and then facilitated the conversion of the released intermediate to androstenedione. Thus, we demonstrated that outer mitochondrial membrane cytochrome b_5 and not microsomal membrane cytochrome b_5 functions as an activator for androgenesis in rat Leydig cells.

Two isoforms of cytochrome b_5 are known to exist in a single cell. One is microsomal cytochrome b_5 (b_5)[1] in the endoplasmic reticulum (ER), and the other is outer mitochondrial membrane cytochrome b_5 (OMb) (1–3). They consist of the following three domains: (*a*) the amino-terminal hydrophilic, (*b*) medial hydrophobic, and (*c*) carboxyl-terminal hydrophilic domains. A protoheme is bound to the first domain, which is highly conserved between b_5 and OMb with 70% identity (4, 5). The hydrophobic domain, consisting of about 20 amino acid residues, is embedded in the lipid bilayer and functions for the insertion of proteins into the membranes as tail-anchored proteins (6). The carboxyl-terminal 10 amino acid residues of b_5 are exposed to the luminal side of the ER cisterna (7, 8) and are required for the targeting of the cytochrome to the organelle (9). The visible spectroscopic properties of the reduced forms are characteristic of the b_5-type hemoproteins. OMb and b_5 are spectrographically indistinguishable from each other due to the highly conserved heme-binding portion (1, 2). OMb and b_5 have a similar mobility on SDS-PAGE and are co-purified unless specific precaution was taken in the purification procedures. Antibodies directed against b_5 that had been purified without the removal step of OMb cross-react with OMb. In some case, cross-reactions are observed even if a highly purified form of OMb or b_5 was immunized in rabbits. These facts made the discrimination between OMb and b_5 difficult. The most convincing way of the discrimination is use of the specific antibodies. We have such antibodies in a large collection of anti-OMb and anti-b_5 antibodies.

Because b_5 is a hemoprotein with sixth co-ordination, it is incapable of activating an oxygen molecule as cytochrome P-450 does. One of its physiological functions is an electron transfer to terminal oxidases such as stearyl-CoA desaturase (10). Some evidence also suggests that b_5 functions as a modifier for some cytochrome P-450-catalyzed reactions although its mechanism is not clear (11, 12). For example, b_5 stimulates the 6β-hydroxylation of testosterone and nifedipine oxidation by recombinant CYP3A4 (13). It also augments C17-C20 lyase activity of pig, guinea pig, and human P-450$_{17\alpha}$ leading to predominant formation of androgens (androstenedione and dehydroepiandrosterone) over 17α-hydroxylated steroids (progesterone and pregnenolone) (14–16). Without involvement of added b_5, the lyase activity of the P-450$_{17\alpha}$ is too low to account for physiological production of androgens *in vivo*.

The physiological functions of OMb are not well understood. The sole experimental evidence for the function is that specific antibodies against rat OMb inhibited semidehydroascorbate reductase, which catalyzes regeneration of half-oxidized ascorbic acid, in outer mitochondrial membrane fractions of rat liver cells (17, 18). In a study on the mechanism for subcellular localization of OMb, we have recently observed that it moves from the outer mitochondrial membrane to the ER membrane in a few hours after administration of dexamethasone, pregnenolone-16α-carbonitrile, or phenobarbital to rats.[2] In tissues other than liver, such as kidney and adrenal glands of rats,

* This work was supported in part grants-in-aid for Scientific Research from the Ministry of Education, Science, Sports and Culture of Japan (to T. O. and A. I.). The costs of publication of this article were defrayed in part by the payment of page charges. This article must therefore be hereby marked "*advertisement*" in accordance with 18 U.S.C. Section 1734 solely to indicate this fact.

‡ To whom correspondence should be addressed. Tel.: 81-92-642-2601; Fax: 81-91-642-2607; E-mail: taogiscc@mbox. nc.kyushu-u.ac.jp.

[1] The abbreviations used are: b_5, microsomal membrane cytochrome b_5; OMb, outer mitochondrial membrane cytochrome b_5; P-450$_{17\alpha}$, cytochrome P-450$_{17\alpha}$ (cytochrome P-450 catalyzing the 17α-hydroxylation and C17-C20 bond cleavage of pregnenolone and progesterone); P-450$_{scc}$, cytochrome P-450$_{scc}$ (cytochrome P-450 catalyzing the side chain cleavage of cholesterol); P-450 reductase, NADPH-cytochrome P-450 reductase; ER, endoplasmic reticulum; PBS, Na-P$_i$-buffered saline; StAR protein, steroidogenic acute regulatory protein; Tricine, *N*-[2-hydroxy-1,1-bis(hydroxymethyl)ethyl]glycine.

[2] K. Abe, J. Kinoshita, T. Ogishima, and A. Ito, manuscript in preparation.

OMb was present in ER in addition to mitochondria. These results indicate that OMb has the potential to be localized either in outer mitochondrial membranes or in ER membranes, although the localization signal of OMb seems to reside in the carboxyl-terminal 10 amino acid residues favorable for mitochondrial targeting (19). In guinea pig, OMb is abundant in adrenal glands, where its localization is exclusively ER. Surprisingly, b_5 is scarcely detected in rat testicular cells, where OMb is distributed almost equally between the outer mitochondrial membranes and ER membranes in considerably high amounts. This suggests that OMb and not b_5 could regulate testicular androgen synthesis by modifying the lyase activity of P-450$_{17\alpha}$. The indistinguishable properties between OMb and b_5 as described above propose a possibility that the stimulatory effects on P-450 that have been believed to be done by b_5 are exerted by OMb. Thus, in this study we analyzed the effects of OMb on rat P-450$_{17\alpha}$, and we found that this cytochrome is a genuine modulator for testicular androgen synthesis in rats.

EXPERIMENTAL PROCEDURES

Animals—Male Sprague-Dawley rats weighing 120–150 g and male Hartley guinea pigs weighing 450–500 g were purchased from Kyudo Co., Ltd. (Kumamoto, Japan). All surgical and experimental procedures were approved and conducted in accordance with the policies of Kyushu University's Animal Care and Use Committee.

Cellular Fractionation and Detection of OMb and b_5—Male Sprague-Dawley rats weighing 120–150 g were intraperitoneally injected with sodium phenobarbital at a dose of 80 mg/kg and killed after 24 h. Liver and testes were removed and homogenized using a Teflon glass homogenizer in ice-cold 10 mM Tris-HCl buffer (pH 7.6) containing 0.25 M sucrose, 0.1 mM EDTA, 2 μg/ml leupeptin, and 2 μg/ml pepstatin A. After the homogenates were centrifuged at 600 × *g* for 10 min, the resultant supernatants were recentrifuged at 6,000 × *g* for 10 min to obtain the mitochondrial fractions. Microsomal fractions were obtained by centrifugation of the post-mitochondrial supernatants at 105,000 × *g* for 60 min. All procedures were done at 4 °C. For analysis of the distribution of OMb and b_5 in the tissues, the subcellular fractions form the tissues and were separated by Tricine/SDS-PAGE (20) and subsequently transferred to polyvinylidene difluoride membranes. The membrane was incubated first with specific anti-rat OMb or anti-rat b_5 IgG and second with goat anti-rabbit IgG-horseradish peroxidase complex, and the immunoreactive bands were finally visualized by chemiluminescence using Western Lighting™ (PerkinElmer Life Sciences).

Enzyme Preparations—All enzyme preparations except as described otherwise were conducted with K-P$_i$ buffer (pH 7.4) containing 20% glycerol, 0.1 mM EDTA, and 0.1 mM dithiothreitol. Rat P-450$_{17\alpha}$ and OMb were solubilized from rat testis microsomes with the 10 mM K-P$_i$ buffer containing 1.4% (w/v) Emulgen 913 (a kind gift from Kao Chemicals, Osaka, Japan) and 2 μg/ml each of leupeptin and pepstatin and after dilution of the detergent to 0.2% absorbed to ω-aminohexyl-Toyopearl column (1.2 × 8.0 cm) equilibrated with 10 mM K-P$_i$ buffer containing 0.2% Emulgen 913. After washing with the 10 mM K-P$_i$ buffer containing 0.2% Emulgen 913, the column was eluted with the 10 mM K-P$_i$ buffer containing 0.2% Emulgen 913 and 0.2% sodium cholate. The eluate contained P-450$_{17\alpha}$. The column was then washed with the 10 mM K-P$_i$ buffer containing 0.4% Emulgen 913 and eluted with the 10 mM K-P$_i$ buffer containing 0.5 M KCl and 0.4% Emulgen 913. The eluate contained OMb. Both enzymes were further purified by high pressure liquid chromatography on a TSK DEAE-5PW column (7.5 × 75 mm, TOSOH, Tokyo, Japan) with a linear gradient of KCl (0–500 mM/60 min) in the 10 mM K-P$_i$ buffer containing 0.4% Emulgen 913. Purified P-450$_{17\alpha}$ was applied to a hydroxylapatite column, and the column was washed extensively with the 10 mM K-P$_i$ buffer without Emulgen 913. The enzyme was eluted from the gel batch with the 400 mM K-P$_i$ buffer containing 10% (w/v) L-α-phosphatidylcholine from egg yolk (Wako Pure Chemical Co. Ltd., Osaka, Japan) and 1% sodium cholate. Proteoliposomes embedded with P-450$_{17\alpha}$ were prepared by a cholate dialysis method as described (21). By using a hydroxylapatite column, detergent-free OMb was also prepared. Rat b_5 was solubilized from liver microsomes and purified with the same method as OMb. NADPH-cytochrome P-450 reductase (P-450 reductase) was solubilized from liver microsomes of phenobarbital-treated rats and purified as described (22). Guinea pig P-450$_{17\alpha}$, OMb, and b_5 were purified from the microsomal fractions of the adrenal glands with the same method as the rat enzyme. The OMb and b_5 were separated from each other by the TSK DEAE-5PW and hydroxylapatite column chromatographies.

Construct of Recombinant OMb and Its Expression in E. coli—An amino-terminal hexahistidine-tagged OMb construct was created by a PCR. The amplified cDNA was inserted into pET-3d vectors at the *Nde*I and *Bam*HI sites to yield pET-hisOMb. BL21 (DE3) strain transformed with pET-hisOMb was cultured for 40 h at 25 °C, and then the transformant was harvested by centrifugation at 1,000 × *g* for 15 min. After sonication the suspension was centrifuged at 177,100 × *g* for 1 h. The pellets were solubilized in 10 mM Hepes-KOH (pH 7.5) buffer containing 20% glycerol and 2% Triton X-100 for 1 h at 4 °C. After centrifugation at 177,100 × *g* for 1 h, the resultant supernatant was applied to a Ni^{2+}-preloaded HisTrap chelating column (1 ml, Amersham Biosciences AB) equilibrated with 10 mM Hepes-KOH (pH 7.5) buffer containing 20% glycerol, 0.1% Triton X-100, 10 mM imidazole, and 0.5 M NaCl. After washed with the equilibrating buffer, the column was eluted with the same buffer except containing 0.5 M imidazole. Because effects of the recombinant OMb on the P-450$_{17\alpha}$-catalyzed reaction were indistinguishable from those of the native forms that were purified from testes and livers, the recombinant OMb was mainly used in this study.

Measurement of 17α-Hydroxylase and C17-C20 Lyase Activities of P-450$_{17\alpha}$—P-450$_{17\alpha}$ containing proteoliposomes were preincubated with P-450 reductase and either OMb or b_5 in a volume of 0.05 ml of 50 mM K-P$_i$ buffer (pH 7.4) containing 20% glycerol, 0.1 mM EDTA, and 0.1 mM dithiothreitol for 60 min at 0 °C. After diluting 10-fold with 20 mM Hepes-NaOH buffer (pH 7.4), progesterone in propylene glycol was added to the reaction mixture. Reaction was started with addition of NADPH at a final concentration of 1 mM and proceeded for 10–20 min at 30 °C. The reaction was stopped by addition of 2 ml of *n*-hexane, and the products were extracted twice with the solvent. After drying under a stream of N_2 gas, the steroids were separated by high pressure liquid chromatography using a COSMOSIL 5SL-II column (4.6 × 150 mm, Nacalai Tesque, Kyoto, Japan) equilibrated and eluted with a solvent (*n*-hexane:2-propanol:acetic acid = 95:5:1). Androstenedione (lyase activity) and 17α-hydroxyprogesterone (17α-hydroxylase activity) were quantified by measuring their absorbance at 240 nm. In some experiments, 17α-hydroxyprogesterone was used as the substrate.

Enzyme and Protein Concentrations—The concentrations of P-450$_{17\alpha}$ were determined spectrophotometrically using a molecular coefficient of 91 $mM^{-1}\cdot cm^{-1}$ for the CO difference spectrum of the reduced form (23). The concentrations of OMb and b_5 were determined from the reduced minus oxidized difference spectrum between 424 and 409 nm by using a molecular coefficient of 185 $mM^{-1}\cdot cm^{-1}$ of b_5 assuming that spectrographic properties of detergent-solubilized forms of OMb and b_5 were indistinguishable from that of a trypsin-solubilized form of b_5 at a Soret band (23, 24). The concentration of P-450 reductase was determined from the absorbance at 455 nm by using a molecular coefficient of 21.4 $mM^{-1}\cdot cm^{-1}$ (25). Amounts of P-450 reductase in rat testis microsomes were analyzed by immunoblotting using anti-rat P-450 reductase-IgG and goat anti-rabbit IgG-horseradish peroxidase complex. The chemiluminescence of the immunoreactive bands was photographed with Light Capture (model AE-6969N, Atto Instruments, Tokyo, Japan) and quantified using CS Analyzer (version 2.0, Atto Instruments). Proteins were determined by a bicinchoninic acid (BCA) method (26).

Immmunohistochemical Localization of OMb and P-450$_{17\alpha}$ in Rat Testis—Testes were excised from adult male rats (Sprague-Dawley) and immediately fixed in 4% paraformaldehyde solution buffered with 10 mM phosphate, pH 7.4, at 4 °C overnight. Fixed tissues were then dehydrated and embedded in paraffin. Three-micron sections were deparaffinized and hydrated using graded alcohol concentrations for standard indirect peroxidase immunohistochemistry. In brief, the preparations were first treated with 0.5% hydrogen peroxide in Na-P$_i$-buffered saline (PBS), pH 7.4, for 20 min at room temperature to block the endogenous peroxidases and then with 5% of normal goat serum in PBS for 20 min at room temperature to block the nonspecific binding. This was followed by overnight incubation at 4 °C with the first antibodies against rat OMb or guinea pig P-450$_{17\alpha}$ that had been incubated with 10% normal rat serum for 60 min at 0 °C. The preparations were then incubated for 2 h at room temperature with horseradish peroxidase-conjugated goat Fab' fragment to rabbit immunoglobulin G (ICN Pharmaceuticals, Inc., Aurora, OH). The immunoreactive proteins were visualized with 3,3'-diaminobenzidine tetrahydrochloride (Sigma) and hydrogen peroxide as described before (27). Nuclear counterstaining was performed using methyl green (Lab Vision Corp., Fremont, CA). For controls, the first antibody, anti-OMb or anti-P-450$_{17a}$ IgG, was omitted from all procedures described above. The antibody against P-450$_{17\alpha}$ was a generous gift from Dr. S. Kominami of Hiroshima University.

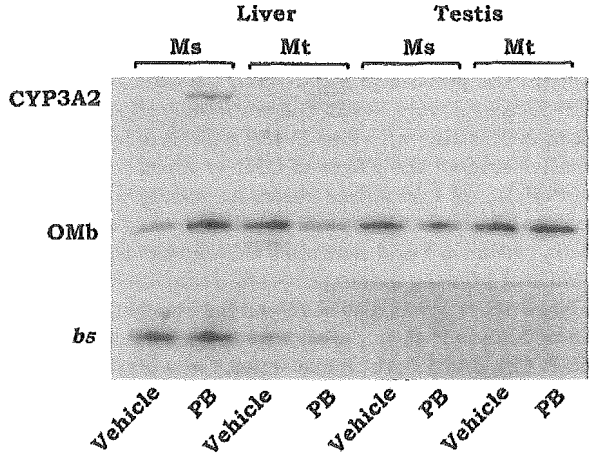

FIG. 1. **Distribution and translocation of OMb and b_5 in rat liver and testis.** Rat liver and testis mitochondria (*Mt*) and microsomes (*Ms*) were isolated, and their proteins (10 μg) were resolved on Tricine/SDS-PAGE (16.5% T, 6% C with 6 M urea). After transferred to polyvinylidene difluoride membranes, proteins were incubated first with specific anti-rat CYP3A2 IgG (Affiniti Research Products Ltd., Exeter, UK), anti-rat OMb IgG, or anti-rat b_5 IgG and then secondarily with anti-rabbit IgG-horseradish peroxidase complex, and finally visualized by chemiluminescence. *PB*, phenobarbital-treated rat.

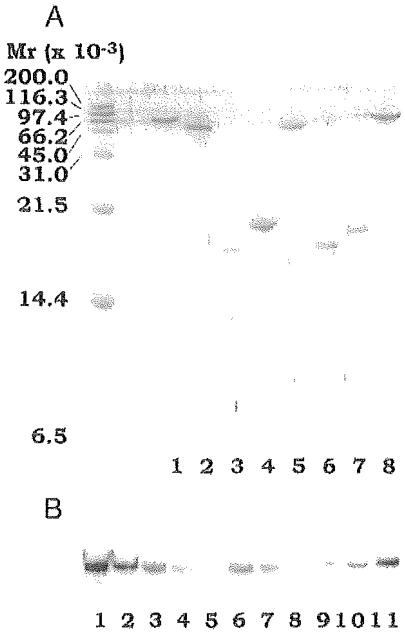

FIG. 2. **Purities of enzymes used in this study and quantification of P-450 reductase in rat testis microsomes.** *A*, P-450 reductase from rat liver microsomes (*lanes 1* and *8*), P-450$_{17\alpha}$ from rat testis microsomes (*lane 2*), b_5 from rat liver microsomes (*lane 3*), recombinant OMb from *E. coli* (*lane 4*), P-450$_{17\alpha}$ (*lane 5*), b_5 (*lane 6*), and OMb (*lane 7*) from guinea pig adrenal microsomes were resolved on Tricine/SDS-PAGE (16.5% T, 6% C with 6 M urea) and stained with Coomassie Brilliant Blue R-250. About 5–20 pmol of purified proteins were electrophoresed. *B*, amounts of P-450 reductase in rat testis microsomes were analyzed by SDS-PAGE (7.5%) and immunoblotting using anti-rat P-450 reductase-IgG and goat anti-rabbit IgG-horseradish peroxidase complex. The chemiluminescence of the immunoreactive bands was quantified with purified P-450 reductase as a standard. The integrated values of the luminescence of the microsomal fractions from two individual rats (*lanes 3–5* and *6–8*, 50, 25, and 12.5 μg of protein, respectively) were calibrated with those of standard bands (*lanes 1, 2,* and *9–11*, 0.25 0.125, 0.0125, 0.025, and 0.1 pmol, respectively). The integration was performed with CS Analyzer (version 2.0, Atto Instruments).

RESULTS

Localization of OMb in Rat Testis Cells—The antibodies used in this study are very specific. No cross-reaction between OMb and anti-b_5 IgG nor between b_5 and anti-OMb IgG was observed if appropriate application of the samples and appropriate dilution of the antibodies were employed. Fig. 1 shows that OMb was distributed between mitochondrial and microsomal fractions almost at a ratio of 1:1 on a protein concentration basis in rat testicular cells, where b_5 was not detected. A large amount of the sample loading on the SDS-PAGE scarcely detected the b_5 band, which is less than 1/100 that of liver cells. Amounts of OMb present in testes were comparable with those in liver per protein. Dual localization (mitochondria and microsomes) of OMb was also observed in the kidneys and adrenal glands (data not shown). Although localization of OMb in the liver cells had been believed to be strictly the outer mitochondrial membrane, translocation of OMb from there to the microsomal membranes was observed at 12 h after administration of phenobarbital to rats. Because this reagent induces not only CYP2A but also CYP3A families, the amount of CYP3A2 was increased in the microsomal fraction. Translocation of OMb to the microsomes was reproduced with other P-450-inducible agents such as dexamethasone, and pregnenolone-16α-carbonitrile (data not shown). Rat OMb thus has a capability to reside in both the outer mitochondrial and microsomal membranes. In the testicular cells, translocation of OMb as manifested in the liver cells was not observed as tested so far by administration of phenobarbital or dexamethasone. In contrast to OMb, b_5 did not change its localization in liver and other cells. Precise results and discussion about the translocation of OMb in liver cells are to be published elsewhere.[2]

Purification of Enzymes Used in This Study—Fig. 2*A* shows the purity of the enzyme preparations used in this study. We purified P-450$_{17\alpha}$ from rat testis microsomes and both b_5 and P-450 reductase from rat liver microsomes. We mainly used a recombinant OMb because this form had the same effects on rat P-450$_{17\alpha}$ with the native form that was purified from the testis microsomes. Use of the recombinant form allowed us to perform the experiments with a constant and sufficient supply of OMb. The data presented herein were collected by using the recombinant OMb instead of the purified OMb. Guinea pig enzymes were purified from the adrenal glands because the P-450$_{17\alpha}$, b_5, and OMb were probably most abundant in the tissue. The specific content of P-450$_{17\alpha}$ in rat testis microsomes was 0.1 nmol/mg protein as determined from the CO difference spectrum. Contribution of P-450$_{scc}$, a mitochondrial protein, to the spectrum is negligible for the microsomal preparation as verified from immunoblotting with anti-P-450$_{scc}$ IgG (data not shown). The specific content of P-450 reductase was determined from the results of Fig. 2*B* to be 1.2 ± 0.3 pmol/mg protein. OMb was present in the testis microsomes at an amount of 0.02–0.05 nmol/mg protein as determined from the reduced minus oxidized difference spectrum. The measurement is, however, not accurate in a crude microsomal fraction with limited amounts of b_5-type protein.

Efficient Electron Transfer Enhances Lyase Activity of P-450$_{17\alpha}$—By using excess amounts of progesterone as the substrate, we can measure both 17α-hydroxylase and lyase activities simultaneously because P-450$_{17\alpha}$ first converts the steroid to the 17α-hydroxylated intermediate, 17α-hydroxyprogesterone, and then the second P-450-catalyzed reaction cleaves the C17-C20 bond to give androstenedione without releasing the intermediate. Kinetic studies employing a rapid quenching method proved that androgen formation from progesterone by guinea pig P-450$_{17\alpha}$ and dehydroepiandrosterone formation from pregnenolone by bovine P-450$_{17\alpha}$ proceeded successively (28, 29). In the successive reaction, rates of release of the intermediate from the substrate-binding pocket in the enzyme and the C–C bond cleavage together with release of the

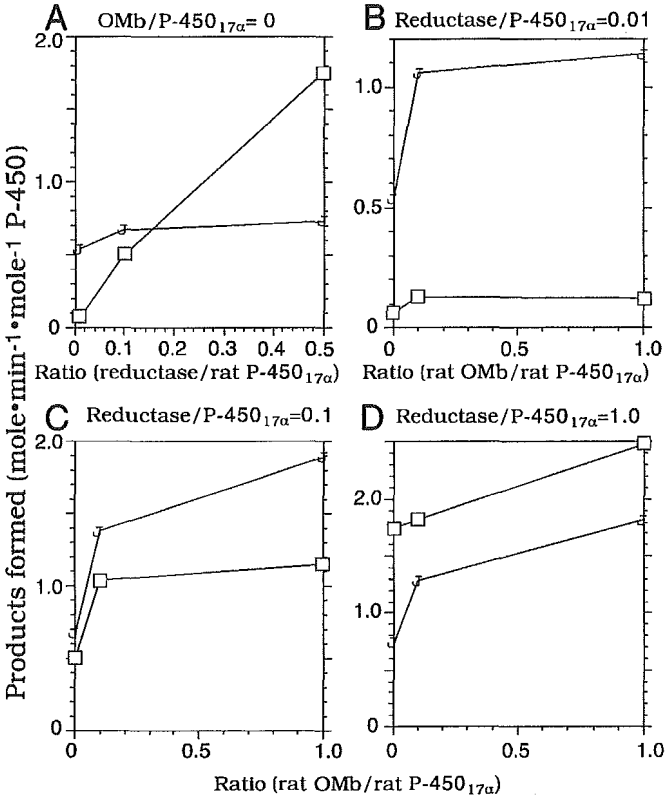

FIG. 3. **Effects of P-450 reductase and OMb on the rat P-450$_{17\alpha}$-catalyzed reactions.** *A*, purified rat P-450$_{17\alpha}$ was incorporated into egg yolk phosphatidylcholine liposomes. The proteoliposomes were incubated with various amounts of P-450 reductase for 60 min at 0 °C. The enzyme reaction was performed, and the products were quantified as described under "Experimental Procedures." *B–D*, the proteoliposomes were incubated with a fixed amount of P-450 reductase and various amounts of OMb for 60 min at 0 °C. The enzyme reaction was performed, and the products were quantified as described under "Experimental Procedures." Molar ratio of P-450 reductase:P-450$_{17\alpha}$, 0.01 (*B*), 0.1 (*C*), and 1.0 (*D*). □, androstenedione; ●, 17α-hydroxyprogesterone.

C17 ketosteroid determine yields of both the 17α-hydroxyl and 17-ketosteroids. Based on this assumption, efficient supply of electrons from P-450 reductase to P-450$_{17\alpha}$ should facilitate the cleavage reaction. This assumption is valid as shown in Fig. 3. Production of androstenedione was increased in a linear fashion with the increase of P-450 reductase added (Fig. 3*A*). The amount of 17α-hydroxyprogesterone produced, however, was constant in the range tested. These indicate that the first hydroxylation step is relatively fast and that the following steps (*i.e.* the release of the intermediate and C-C bond cleavage) are rate-limiting as shown previously (28). The increase of the electron transfer should enhance the second P-450-catalyzed reaction (*i.e.* C17-C20 bond cleavage) leading to androstenedione formation without affecting the release of the intermediate. The lyase activity was about 1/10th the 17α-hydroxylase activity at a low ratio of P-450 reductase to P-450$_{17\alpha}$ (reductase:P-450$_{17\alpha}$ of 1:100), and it was more than 2.5 times the 17α-hydroxylase activity at a ratio of P-450 reductase to P-450$_{17\alpha}$ of 0.5. Obviously, rat P-450$_{17\alpha}$ has a lyase activity that is higher than the 17α-hydroxylase activity compared with the guinea pig enzyme (see Refs. 28 and 30 and see the text below).

Effects of OMb and b_5 on 17α-Hydroxylase and Lyase of Rat P-450$_{17\alpha}$—Addition of OMb to the P-450$_{17\alpha}$-dependent reaction system enhanced both the 17α-hydroxylase and lyase activities over the range of ratios of P-450 reductase to P-450$_{17\alpha}$ tested. The stimulatory effects, however, tended to be saturated at a low ratio of OMb to P-450$_{17\alpha}$ when the electron transfer was slow due to a low concentration of P-450 reductase (compare the profiles in Fig. 3, *B–D*). Because the amount of the reductase is very low in the testis microsomes as revealed by immunoblotting with anti-P-450 reductase IgG (Fig. 2*B*), we hereafter studied the effects of OMb at a ratio of P-450 reductase:P-450$_{17\alpha}$ of 1:50 unless otherwise mentioned. OMb stimulated the 17α-hydroxylase activity linearly at ratios of OMb to P-450$_{17\alpha}$ below 0.1 and continued to increase it gradually up to the ratio of 1.0 to an extent of 7–8-fold (Fig. 4*A*). Stimulation of the lyase activity was also observed but reached a plateau at a ratio of OMb to P-450$_{17\alpha}$ of about 0.1. Above the molar ratio of OMb:P-450$_{17\alpha}$ of 1.0, the lyase activity was almost constant up to the ratio of 2.0, whereas the 17α-hydroxylase activity continued to increase gradually (data not shown). Maximum stimulation of the lyase activity by OMb was about 3-fold. Addition of b_5 to the reaction system containing P-450$_{17\alpha}$ and P-450 reductase also augmented both lyase and 17α-hydroxylase activities but with a manner different than that of OMb (Fig. 4*B*). It stimulated the lyase activity to an extent similar to that of OMb (3-fold) at ratios of b_5 to P-450$_{17\alpha}$ of 0.2–0.5, whereas it enhanced the 17α-hydroxylase activity about twice at the most. At the high ratio, the 17α-hydroxylase and lyase activities dropped to the same value and one-third of the original (without b_5) activity, respectively (Fig. 4*B*), and further decreased above the ratio of 1.0 (data not shown). The differences in the stimulatory effects between OMb and b_5 were apparent when the 17α-hydroxylase:lyase activity ratio was plotted in the *y* axis (Fig. 4*C*). OMb had a tendency to elevate preferentially the 17α-hydroxylase, whereas b_5 stimulated the lyase preferentially. A rise of the 17α-hydroxylase:lyase at a ratio of b_5 to P-450$_{17a}$ of 1.0 was due to the strong inhibitory effect on the lyase in a high concentration of b_5 relative to P-450$_{17\alpha}$.

Effects of OMb and b_5 on 17α-Hydroxylase and Lyase of Guinea Pig P-450$_{17\alpha}$—In general, P-450$_{17\alpha}$ of most animals has strong 17α-hydroxylase and weak lyase activities in the absence of b_5 except murine P-450$_{17\alpha}$. In the guinea pig P-450$_{17\alpha}$-catalyzed reaction, b_5 has been reported to stimulate the lyase activity without significant elevation of the 17α-hydroxylase activity (30). We purified b_5 and OMb from microsomes of guinea pig adrenals and analyzed the effects of these proteins toward the P-450$_{17\alpha}$ that had also been purified from the same membrane preparations and embedded in proteoliposomes. Rat b_5 greatly stimulated the lyase activity up to a ratio of b_5 to guinea pig P-450$_{17\alpha}$ of 0.5 together with slight activation of the 17α-hydroxylase. However, it reduced both activities at the high ratio (Fig. 5*B*). The stimulatory profile of rat b_5 on guinea pig P-450$_{17\alpha}$ was essentially the same on rat P-450$_{17\alpha}$ except that activation of the lyase was more dominant than that of the 17α-hydroxylase and that the maximum stimulation of both activities occurred at lower ratios, b_5:P-450$_{17\alpha}$ of 0.05–0.1. At a ratio of rat b_5 to guinea pig P-450$_{17\alpha}$ of 0.5, the increase in the lyase activity was about 6-fold and that of the 17α-hydroxylase was 1.5-fold. Guinea pig b_5 also greatly stimulated the lyase activity up to the ratio of 0.5, where the activity was 6-fold and the effect reached a plateau (Fig. 5*E*). The 17α-hydroxylase activity continued to increase up to a ratio of guinea pig b_5 to guinea pig P-450$_{17\alpha}$ of 1.0. In contrast, the stimulatory effect of rat OMb on guinea pig P-450$_{17\alpha}$ was not observed over the range measured (Fig. 5*A*). Only activation of the 17α-hydroxylase was observed in an OMb-dependent manner up to a ratio of rat OMb to guinea pig P-450$_{17\alpha}$ of 0.5, where stimulation was about 3.5-fold. The effect of guinea pig OMb on guinea pig P-450$_{17\alpha}$ was intermediate between those of rat OMb and guinea pig b_5 (Fig. 5*D*). Guinea pig OMb stimulated the 17α-hydroxylase and lyase activities about 3- and 4.5-fold, respec-

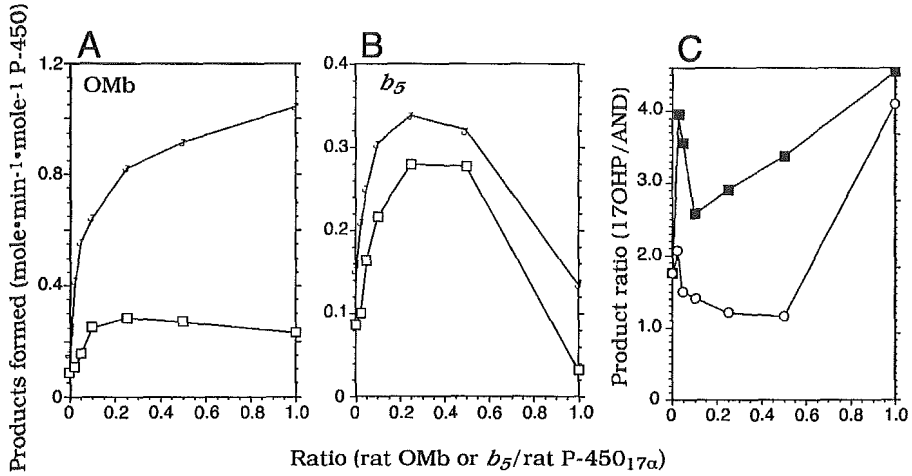

FIG. 4. **Effects of rat OMb and b_5 on rat P-450$_{17\alpha}$-catalyzed reactions.** The P-450$_{17\alpha}$-containing proteoliposomes were incubated with P-450 reductase (0.02 eq) and various amounts of OMb (*A*) and b_5 (*B*) for 60 min at 0 °C. The enzyme reaction was performed, and the products were quantified as described under "Experimental Procedures." □, androstenedione; ●, 17α-hydroxyprogesterone. The product ratio of 17α-hydroxyprogesterone:androstenedione was plotted (*C*). *17OHP*, 17α-hydroxyprogesterone; *AND*, androstenedione. The values in the presence of OMb (■) and b_5 (○) are shown.

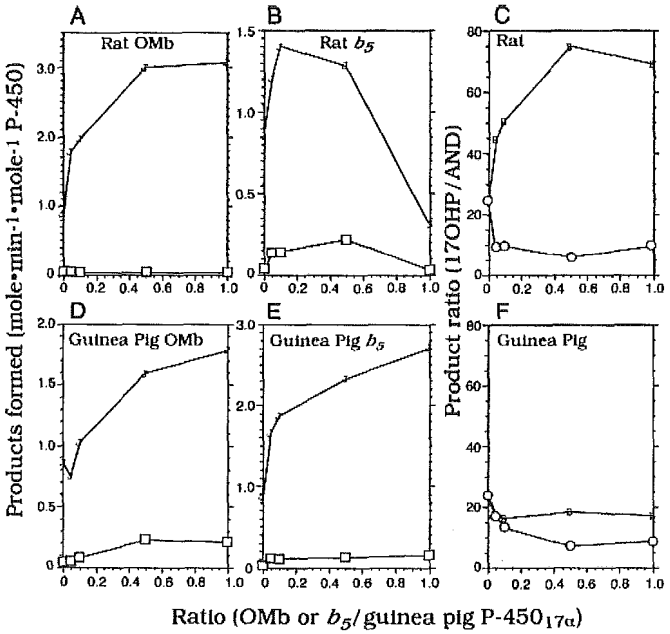

FIG. 5. **Effects of OMb and b_5 on guinea pig P-450$_{17\alpha}$-catalyzed reactions.** The guinea pig P-450$_{17\alpha}$-containing proteoliposomes were incubated with P-450 reductase (0.02 eq) and various amounts of rat OMb (*A*), rat b_5 (*B*), guinea pig OMb (*D*), and guinea pig b_5 (*E*) for 60 min at 0 °C. The enzyme reaction was performed, and the products were quantified as described under "Experimental Procedures." □, androstenedione; ●, 17α-hydroxyprogesterone. The product ratio of 17α-hydroxyprogesterone:androstenedione was plotted for the rat enzymes (*C*) and guinea pig enzymes (*F*). *17OHP*, 17α-hydroxyprogesterone; *AND*, androstenedione. The values in the presence of OMb (■) and b_5 (○) are shown.

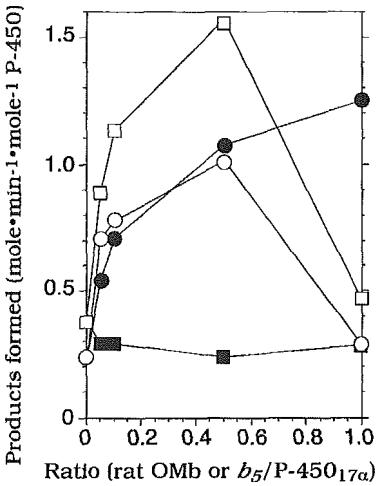

FIG. 6. **Effects of rat OMb and b_5 on lyase activity of P-450$_{17\alpha}$ toward 17α-hydroxyprogesterone.** The rat P-450$_{17\alpha}$-containing proteoliposomes were incubated with P-450 reductase and rat OMb (●) or rat b_5 (○) for 60 min at 0 °C. The guinea pig P-450$_{17\alpha}$-containing proteoliposomes were incubated with P-450 reductase and rat OMb (■) or rat b_5 (□) for 60 min at 0 °C. The enzyme reaction was performed with 0.1 mM of 17α-hydroxyprogesterone for 20 min, and the products were quantified as described under "Experimental Procedures."

tively, at a ratio of OMb:P-450$_{17\alpha}$ of 1:1. There is a more distinct difference in the 17α-hydroxylase:lyase ratio between the stimulatory effects on guinea pig P-450$_{17\alpha}$ by rat OMb and b_5 (Fig. 5*C*).

Effects of OMb and b_5 on Lyase Activity toward 17α-Hydroxyprogesterone—We then directly analyzed the C17-C20 lyase activities toward 17α-hydroxyprogesterone using the steroid as the substrate (Fig. 6). Rat b_5 augmented the lyase activity of rat P-450$_{17\alpha}$ up to a ratio of b_5 to P-450$_{17\alpha}$ of 0.5 about 4-fold, but the activity drastically dropped at the ratio of 1.0. Such a stimulatory profile was essentially the same on guinea pig P-450$_{17\alpha}$ by rat b_5. Rat OMb stimulated the lyase activity as the ratio to rat P-450$_{17\alpha}$ increased, and the activation reached 5-fold at the ratio of 1.0. As shown in the successive reaction with an excess amount of progesterone (Fig. 5*A*), the inability of rat OMb to exert a stimulatory effect on the lyase activity of guinea pig P-450$_{17\alpha}$ toward 17α-hydroxyprogesterone was reproduced.

Effect of OMb on P-450$_{17\alpha}$-catalyzed Reaction at a Low Concentration of Progesterone—The experiments on the effects of OMb and b_5, which were described above, were performed with a saturating concentration of progesterone (0.1 mM). Under this condition, we measured initial velocities of both 17α-hydroxylase activity and successive 17α-hydroxylase and C17-C20 lyase activities of P-450$_{17\alpha}$ at the same time. We then conducted the P-450$_{17\alpha}$-catalyzed reaction at a low concentration of progesterone. Under such a condition, a mixture of the successive reaction and two-step reaction would proceed, *i.e.* at the first step 17α-hydroxylation of progesterone and subsequent release of 17α-hydroxyprogesterone from the enzyme pocket and at the second step reincorporation of the intermediate and

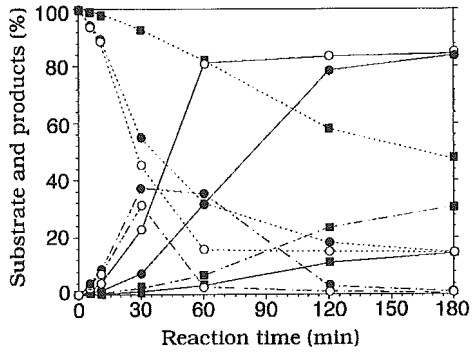

FIG. 7. **Effects of rat OMb and b_5 on product formation by rat P-450$_{17\alpha}$ with a low concentration of progesterone.** The rat P-450$_{17\alpha}$–containing proteoliposomes were incubated with P-450 reductase (■), P-450 reductase and rat OMb (●) or P-450 reductase and rat b_5 (○) for 60 min at 0 °C. The ratio of P-450 reductase was 0.02 and those of OMb and b_5 were 0.5 to P-450$_{17\alpha}$. The enzyme reaction was performed with 1.5 μM of progesterone for 180 min, and the products were quantified as described under "Experimental Procedures." The amounts of the substrate and products as described by percentage of the added progesterone *versus* the reaction time were plotted. Progesterone (- - -), 17α-hydroxyprogesterone (- - - -), and androstenedione (—).

its C17-C20 cleavage. At 1.5 μM progesterone, rat P-450$_{17a}$ alone produced a small amount of androstenedione together with a little more 17α-hydroxyprogesterone (Fig. 7). In the presence of rat OMb (0.5 eq), P-450$_{17a}$ rapidly converted progesterone mainly to 17α-hydroxyprogesterone and secondly to androstenedione reflecting the product ratio under an excess amount of progesterone as shown in Fig. 4*A*. The amount of 17α–hydroxyprogesterone was constant between 30 and 60 min, during which period the input and output were equilibrated and then started to decline, and the intermediate was finally almost consumed. The rate of decrease of progesterone became slow after 60 min and seemed to have stopped at 120 min. On the other hand, production of androstenedione accelerated after 30 min and persisted up to 120 min, at which time point most of the substrate and intermediate were consumed. Addition of rat b_5 to the P-450$_{17\alpha}$-catalyzed reaction system stimulated productions of 17α-hydroxyprogesterone as much as that of OMb during the first 30-min reaction and facilitated a rapid consumption of the intermediate after 30 min. It enhanced androstenedione formation more than that of OMb at the first 30-min reaction, and the formation accelerated to 60 min and had almost stopped by that time probably because of exhaustion of usable substrates (progesterone and 17α-hydroxyprogesterone). The reason for a significant amount of progesterone remaining even after 180 min of incubation could be attributed to an inhibitory effect of androstenedione on the P-450$_{17\alpha}$-catalyzed reaction. Although androstenedione formation facilitated by b_5 was faster than that by OMb, amounts of the product at 120 min were almost equal. After the reaction for 180 min, the androstenedione formation stimulated by OMb was more than five times that by P-450$_{17\alpha}$ alone. Effects of rat OMb and b_5 on guinea pig P-450$_{17\alpha}$ were also examined in the reactions at a low concentration of progesterone. Rat b_5 stimulated androstenedione formation by guinea pig P-450$_{17\alpha}$ in a fashion similar to that by rat P-450$_{17\alpha}$. In contrast, rat OMb did not exert any stimulatory effects on the production despite a significant activation of 17α-hydroxyprogesterone production (data not shown).

Localization OMb in Leydig Cells of Rat Testis—Because testicular cells are heterogeneous, the following question arises: Is OMb really present in the steroidogenic cells, *i.e.* Leydig cells? To solve this, we conducted immunohistochemical analysis using anti-rat OMb IgG on the rat testis. OMb as well as P-450$_{17\alpha}$ was only detected in Leydig cells; no positive reactions were observed in Sertoli cells, spermatogonia, spermatocytes, spermatids, and spermatozoa (Fig. 8). In contrast, cells were not significantly stained with anti-rat b_5 IgG (data not shown). Localization of OMb in Leydig cells was also confirmed with the guinea pig testis (data not shown).

DISCUSSION

Although the roles of OMb have not been known, those of b_5 are considerably well known. They are as follows: (*a*) transfer of electrons from NADH to desaturases such as stearoyl-CoA desaturase (10) and Δ7-sterol 5-desaturase (31); (*b*) NADH-dependent reduction of methemoglobin to regenerate hemoglobin (32), and (*c*) stimulation of some P-450-dependent oxygenation. The intracellular localization of b_5 is absolutely ER, whereas that of OMb is variable between outer mitochondrial and ER membranes from cells to cells or animals to animals. Furthermore, OMb changes its localization at least in hepatic cells under different conditions (Fig. 1). In Leydig cells of rat testes, OMb is distributed between outer mitochondrial and ER membranes. In contrast, b_5, which is believed to be responsible for stimulation of the P-450$_{17\alpha}$ of several animals other than rats in efficient production of androgen, is scarcely detectable in rat testicular cells. In the present study, we analyzed the effects of rat OMb on P-450$_{17\alpha}$ purified from rat testis microsomes using a reconstituted system with proteoliposomes. This system is believed to provide membrane proteins with a reaction field comparable with the biomembrane environment and allowed us to perform quantitative analyses in such a way as controlling the enzyme, modulator, and substrate concentrations. Androgen syntheses from progesterone by guinea pig P-450$_{17\alpha}$ (28) and from pregnenolone by bovine P-450$_{17\alpha}$ (29) are proven to proceed by a successive reaction in the presence of excess amounts of progesterone, in which efficient electron supplies from P-450 reductase to P-450 facilitate the C17-C20 cleavage reaction of the 17α-hydroxylated intermediates bound to the enzyme pocket. The stimulatory effect of OMb on rat P-450$_{17\alpha}$–catalyzed reactions was also observed (Fig. 3). In the rat testis, the amount of P-450 reductase, however, is limited, *i.e.* from 1/50 to 1/100 of P-450$_{17\alpha}$ (Fig. 2). We thus analyzed the effects of b_5 and OMb at a ratio of reductase:P-450 of 0.02:1.0 assuming that the physiological electron transfer between the reductase and P-450 in the rat testis ER operates at about this ratio. Although different from the P-450$_{17\alpha}$ of other animals, the lyase activity is higher than the 17α-hydroxylase activity in rat P-450$_{17\alpha}$ if sufficient electrons are supplied, it becomes drastically reduced under the physiological concentration of P-450 reductase. In such a low concentration of P-450 reductase, androgen production is very slow probably due to the dominant release of the 17α-hydroxylated intermediate from the enzyme pocket, which becomes relatively faster than the second two-electron transfers needed for the C17-C20 cleavage reaction. Androstenedione produced at an initial rate from a saturation amount of progesterone by rat P-450$_{17\alpha}$ in the presence of the physiological concentration of P-450 reductase is very small in the absence of b_5 or OMb (Fig. 4). Moreover, the majority of products from progesterone is 17α-hydroxyprogesterone, which is about twice of androstenedione (Fig. 4) and assumed not to be converted to androstenedione in the presence of an excess amount of progesterone in the successive reaction model (29). Rat b_5 from the liver virtually acted on the P-450$_{17\alpha}$ by compensating for the limited reduction. It elevated the lyase activity to a level corresponding to that at a ratio of P-450 reductase: P-450 of 0.1:1.0 in the absence of b_5. This effect is, however, saturated at a low ratio of b_5 to P-450$_{17\alpha}$ and even inhibitory to the P-450$_{17\alpha}$–catalyzed reaction at the high ratios if the amount of P-450 reductase in the reaction system is limited. The reason for such an inhibitory action of b_5 is unclear but

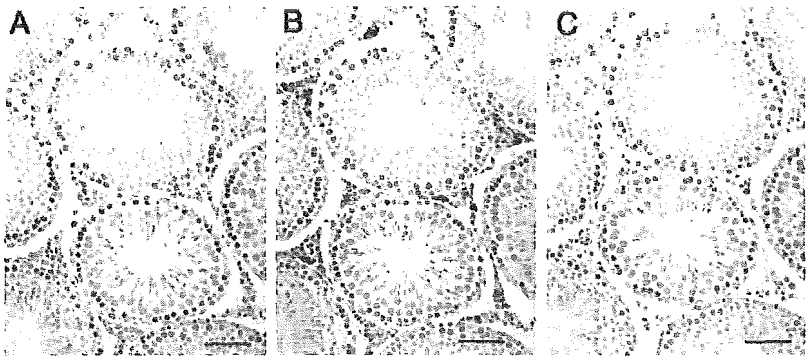

FIG. 8. **Localization of OMb in Leydig cells of rat testis.** Paraffin sections (3 μm) of a male rat testis were reacted with anti-rat OMb IgG (*A*), anti-guinea pig P-450$_{17a}$ IgG (*B*), or a control IgG (*C*). The immunoreactive proteins were visualized with 3,3′-diaminobenzidine tetrahydrochloride. *Bars*, 50 μm.

could be attributed to some interaction of b_5 with the reductase or even with P-450$_{17\alpha}$ in a complicated manner. Rat OMb also showed stimulatory effects on rat P-450$_{17\alpha}$ with some different manners. The lyase activity was increased linearly to the amount of OMb at low ratios of OMb to P-450$_{17\alpha}$ and reached a constant around the ratio of 0.2 without a significant decrease at the high ratios. Increase in the 17α-hydroxylase activity was larger than that in the lyase activity, and the increase curve also tended to saturate around the ratio of 0.2 but proceeded gradually to the ratio of 1.0 and more. Differences of the stimulation profiles for P-450$_{17\alpha}$ between b_5 and OMb was more obvious when they were evaluated for effects on guinea pig P-450$_{17\alpha}$, which has a very high 17α-hydroxylase activity relative to the lyase activity. The effects of rat b_5 were essentially the same for rat P-450$_{17\alpha}$, whereas rat OMb only activated the 17α-hydroxylase activity without elevation of the lyase activity. Although a reaction system of guinea pig P-450$_{17\alpha}$ with rat b_5 or rat OMb is non-physiological, it disclosed differences of the effects of two similar hemoproteins clearly.

In rat testicular cells, OMb is present nearly equally in both the mitochondria and microsomes with a concentration comparable with that in liver mitochondria. By immunohistochemical analyses, the rat testicular OMb was localized in Leydig cells, where P-450$_{17\alpha}$ coexisted. In contrast, we scarcely detected b_5 in the rat testis microsomes, not to mention its presence in the mitochondria, by cell fractionation. Immunohistochemical analysis using anti-rat b_5 IgG did not detect significant staining of b_5 in Leydig cells.

There have been numerous reports on stimulation of b_5 on P-450$_{17\alpha}$ except rat enzymes employing various assay systems (14–16, 33). Most of them confirmed the function as a stimulator for the lyase. There is no study, however, on involvement of OMb in the androgen synthesis except a recent one on human OMb (type 2 cyt-b_5) and P-450$_{17\alpha}$ both expressed transiently in HEK-293c cells (34). In the present study employing enzymatic and cell biological analyses, we were able to demonstrate the role of OMb and not b_5 as a physiological modulator for rat testicular P-450$_{17\alpha}$. Although rat OMb preferentially stimulates 17α-hydroxyprogesterone production from progesterone, it should be an activator for androgen synthesis by P-450$_{17\alpha}$. In an excess amount of progesterone, rat P-450$_{17\alpha}$ produces androstenedione by the successive reaction from the substrate. This situation, however, could not be feasible under physiological conditions. In steroidogenic cells, cholesterol, the precursor of steroidogenesis, is supplied from a pool in the outer mitochondrial membrane to the inner membrane where P-450$_{SCC}$ is present through action of steroidogenic acute regulatory (StAR) protein (35). Activation of StAR protein is triggered by the stimulus of pituitary hormones such as luteinizing hormone and ACTH. The cholesterol is rapidly converted to pregnenolone by the rate-limiting enzyme, P-450$_{SCC}$, and the pregnenolone is then oxidized by 3β-hydroxysteroid dehydrogenase to give a transient increase of progesterone. The produced progesterone is promptly consumed to the lower stream products because steroidogenetic enzyme systems in general have no rate-limiting step other then the side chain cleavage. Such a flow of steroids would be reflected by the reaction condition with a low amount of progesterone as conducted in the experiment of Fig. 7. At a low concentration of progesterone, OMb stimulates rat P-450$_{17\alpha}$ to produce both 17α-hydroxyprogesterone and androstenedione, in which 17α-hydroxyprogesterone production is preferential. As the result, 17α-hydroxyprogesterone accumulates and then serves as the second but main substrate. The intermediate steroid is then converted to androstenedione, which process is also stimulated by OMb. Although the rate of androgen production stimulated by b_5 is about twice as fast as that by OMb, the amount at 120–180 min was nearly the same for both hemoproteins. A question then arises as to why OMb and not b_5 acts as the modulator for androgen production in the rat testis. One reason could be the inhibitory effects of b_5 on P-450$_{17\alpha}$ at a high ratio of b_5 per P-450$_{17\alpha}$. In this respect, OMb does not inhibit P-450$_{17\alpha}$ activity at the ratio of 1.0. The early study by Onoda and Hall (14) pointed out difference of the effects between pig liver and newborn testis b_5 on androgen production in adult pig testis microsomes. The testicular b_5 stimulated concentration-dependently the lyase activity, whereas the liver b_5 had an optimum concentration for the maximum stimulation. Rat OMb has a tendency to stimulate preferentially the 17α-hydroxylase activity of P-450$_{17\alpha}$. In fact, rat P-450$_{17\alpha}$ has a week 17α-hydroxylase activity relative to the P-450$_{17\alpha}$ of other animals. A high 17α-hydroxylase activity is necessary for cortisol production by other animals than murines, which do not produce cortisol due to the absence of P-450$_{17\alpha}$ in the adrenal glands. Preferential stimulation of the 17α-hydroxylase activity by rat OMb suggests that the considerably high 17α-hydroxylase should be needed for an unknown reason in Leydig cells. Finally, the mobile property of OMb in rat liver cells (Fig. 1) could also have a physiological role as a modulator that transfers between mitochondria (inactive) and ER (active) in Leydig cells, although we have not analyzed translocation of OMb in rat testicular cells.

There are essentially two possible explanations for the stimulatory effects of b_5 on some P-450-catalyzed reactions. One is that b_5 is involved in the second electron transfer during the P-450 reaction cycle. The participation in the first electron transfer is not practical because the redox potential of the ferric state of P-450 is lower than that of the ferrous state of b_5. For the electron transfer hypothesis, the stimulatory effect of apo-b_5 on testosterone 6β-hydroxylation and nifedipine oxida-

tion by CYP3A4, however, disapproved (16). A second explanation is to give P-450 conformational changes through complex formation between the P-450 and b_5. Thus, the P-450 obtains a stimulated catalytic activity in the complex. The stimulatory profile of P-450$_{17\alpha}$ activities in the presence of b_5 thus suggests some interaction between these proteins but with complexity (Figs. 4*B* and 5*B*). The effect of the amount of P-450 reductase on the lyase activity of P-450$_{17\alpha}$ in the present study (Fig. 3*A*) does not seem in conflict with the first hypothesis. The more efficiently the electrons are supplied, the more rapidly the second P-450-catalyzed reaction (C17-C20 cleavage) proceeds, and thereby production of androstenedione overtakes the release of 17α-hydroxyprogesterone from the enzyme pocket. The effects of OMb in the preferential elevation of 17α-hydroxylation, however, are not accountable with the first hypothesis because the efficient electron supply would not facilitate the release of 17α-hydroxyprogesterone. Yamazaki *et al.* (29) reported that the release of the intermediate (17α-hydroxyprogesterone), the C17-C20 cleavage reaction, and the release of the final product (androstenedione) are all very slow relative to the first 17α-hydroxylation. This means that 17α-hydroxylase and lyase activities are mainly determined by the rate of the intermediate release and the rates of the C-C bond cleavage and final product release, respectively. If the first hydroxylation step (17α-hydroxylation) is fast, the overall rate does not change even if the first step is influenced by OMb or b_5. Thus, at least the increase of the rate for the release of 17α-hydroxyprogesterone is impractical by activation of the electron transfer. It is likely that rat OMb has abilities to facilitate the release of 17α-hydroxyprogesterone and C17-C20 cleavage reaction and/or release of androstenedione.

This is the first demonstration of the physiological role of OMb. The functions in other tissues as well as the mechanism and function of the translocation between mitochondria and ER should be elucidated.

REFERENCES

1. Fukushima, K., Ito, A., Omura, T., and Sato, R. (1972) *J. Biochem. (Tokyo)* **71,** 447–461
2. Ito, A. (1980) *J. Biochem. (Tokyo)* **87,** 63–71
3. Ito, A. (1980) *J. Biochem. (Tokyo)* **87,** 73–80
4. Lederer, F., Ghrir, R., Guiard, B., Cortial, S., and Ito, A. (1983) *Eur. J. Biochem.* **132,** 95–102
5. De Silvertis, M., D'Arrigo, A., and Borgese, N. (1995) *FEBS Lett.* **370,** 69–74
6. Kutay, U., Ahnert-Hilgen, G., Hartmann, E., Wiedenmann, B., and Rapoport, T. A. (1995) *EMBO J.* **14,** 217–223
7. Vergeres, G., Ramsden, J., and Waskell, L. (1995) *J. Biol. Chem.* **270,** 3414–3422
8. Kuroda, R., Kinoshita, J., Honsho, M., Mitoma, J., and Ito, A. (1996) *J. Biochem. (Tokyo)* **120,** 828–833
9. Mitoma, J., and Ito, A. (1992) *EMBO J.* **11,** 4197–4203
10. Ozols, J. (1976) *Ann. Clin. Res.* **8,** 182–192
11. Hilderbrandt, A., and Estabrook, R. W. (1971) *Arch. Biochem. Biophys.* **143,** 66–79
12. Guengerich, F. P., Martin, M. V., Beaune, P. H., Kremers, P., Wolff, T., and Waxman, D. J. (1986) *J. Biol. Chem.* **261,** 5051–5060
13. Yamazaki, H., Useng, Y.-F., Shimada, T., and Guengerich, F. P. (1995) *Biochemistry* **34,** 8380–8383
14. Onoda, M., and Hall, P. F. (1982) *Biochem. Biophys. Res. Commun.* **108,** 454–460
15. Kominami, S., Ogawa, N., Morimune, R., Huang, D. Y., and Takemori, S. (1992) *J. Steroid Biochem. Mol. Biol.* **42,** 57–64
16. Auchus, R. J., Lee, T. C., and Miller, W. L. (1998) *J. Biol. Chem.* **273,** 3158–3165
17. Ito, A., Hayashi, S., and Yoshida, T. (1981) *Biochem. Biophys. Res. Commun.* **101,** 591–598
18. Nishino, H., and Ito, A. (1986) *J. Biochem. (Tokyo)* **100,** 1523–1531
19. Kuroda, R., Ikenoue, T., Honsho, M., Tujimoto, S., Mitoma, J., and Ito, A. (1998) *J. Biol. Chem.* **273,** 31097–31102
20. Schägger, H., and von Jagow, G. (1987) *Anal. Biochem.* **166,** 368–379
21. Kominami, S., Inoue, S., Higuchi, A., and Takemori, S. (1989) *Biochim. Biophys. Acta* **985,** 293–299
22. Kominami, S., Ogishima, T., and Takemori, S. (1982) in *Flavins and Flavoproteins* (Massey, V., and Williams, C. H., eds) pp. 715–718, Elsevier North-Holland Inc., Amsterdam
23. Omura, T., and Sato, R. (1964) *J. Biol. Chem.* **239,** 2370–2378
24. Omura, T., and Takesue, S. (1970) *J. Biochem. (Tokyo)* **67,** 249–257
25. French, J. S., and Coon, M. J. (1979) *Arch. Biochem. Biophys.* **195,** 565–577
26. Smith, P. K., Krohn, R. I., Hermanson, G. T., Millia, A. K., Gartner, F. H., Provenzano, M. P., Fujimoto, E. K., Goeke, N. M., Olson, B. J., and Klenk, D. C. (1985) *Anal. Biochem.* **150,** 76–85
27. Ogishima, T., Suzuki, H., Hata, J., Mitani, F., and Ishimura, Y. (1992) *Endocrinology* **130,** 2971–2977
28. Tagashira, H., Kominami, S., and Takemori, S. (1995) *Biochemistry* **34,** 10939–10945
29. Yamazaki, T., Ohno, T., Sakaki, T., Akiyoshi-Shibata, M., Yabusaki, Y., Imai, T., and Kominami, S. (1998) *Biochemistry* **37,** 2800–2806
30. Shinzawa, K., Kominami, S., and Takemori, S. (1985) *Biochim. Biophys. Acta* **833,** 151–160
31. Kawata, S., Trzaskos, J. M., and Gaylor, J. L. (1985) *J. Biol. Chem.* **260,** 6609–6617
32. Abe, K., and Sugita, Y. (1979) *Eur. J. Biochem.* **101,** 423–428
33. Guryev, P. L., Gilep, A. A., Usanov, S. A., and Estabrook, R. W. (2001) *Biochemistry* **40,** 5018–5031
34. Soucy, P., and Luu-The, V. (2002) *J. Steroid Biochem. Mol. Biol.* **80,** 71–75
35. Stocco, D. M., and Clark, B. J. (1996) *Endocr. Rev.* **17,** 221–244

THE JOURNAL OF BIOLOGICAL CHEMISTRY
Vol. 278, No. 19, Issue of May 9, pp. 17084–17092, 2003
Printed in U.S.A.

An Inverse Correlation between Expression of a Preprocathepsin B-related Protein with Cysteine-rich Sequences and Steroid 11β-Hydroxylase in Adrenocortical Cells*

Received for publication, February 11, 2003
Published, JBC Papers in Press, February 24, 2003, DOI 10.1074/jbc.M301477200

Kuniaki Mukai‡§, Fumiko Mitani‡, Hideko Nagasawa‡¶, Reiko Suzuki‡, Tsuneharu Suzuki‡‖, Makoto Suematsu‡, and Yuzuru Ishimura‡**

From the ‡Department of Biochemistry and Integrative Medical Biology, School of Medicine, Keio University, 35 Shinanomachi, Shinjuku-ku, Tokyo 160-8582 and ‖Minophagen Pharmaceutical Co., 2-2-3 Komatsubara, Zama, Kanagawa 228-0002, Japan

A cDNA encoding a secretory protein hitherto unknown was cloned from mouse adrenocortical cells by subtractive hybridization between the cells without and with expressing steroid 11β-hydroxylase (Cyp11b-1), a marker for the functional differentiation of cells in the zonae fasciculata reticularis (zFR). The deduced protein consisting of 466 amino acids contained a secretory signal, epidermal growth factor-like repeats, and a proteolytically inactive cathepsin B-related sequence. The amino acid sequence was 89% identical with that of human tubulointerstitial nephritis antigen-related protein. Among the mouse organs examined, adrenal glands prominently expressed its mRNA. The mRNA and its encoded protein were detected in the outer adrenocortical zones that do not express Cyp11b-1, *i.e.* the zona glomerulosa and the undifferentiated cell zone, while being undetectable in zFR that express Cyp11b-1. The new protein was designated as adrenocortical zonation factor 1 (AZ-1). Clonal lines with different levels of AZ-1 expression were established from Y-1 adrenocortical cells that originally express Cyp11b-1 but little AZ-1. Analyses of the clonal lines revealed that Cyp11b-1 is detected in the clonal lines maintaining little AZ-1 expression and becomes undetectable in those expressing AZ-1. On the other hand, irrespective of the AZ-1 expression, all clones expressed cholesterol side-chain cleavage enzyme, which occurs throughout the cortical zones. These results demonstrated that adrenocortical cells expressing AZ-1 do not express Cyp11b-1, whereas those with little AZ-1 express this zFR marker *in vitro* and *in vivo*, implying a putative role of AZ-1 in determining the zonal differentiation of adrenocortical cells.

The adrenal cortex of mammals consists of three major zones that contain both functionally and morphologically distinct cells; they are the zona glomerulosa (zG),[1] the zona fasciculata (zF), and the zona reticularis (1). The cells in zG, the outermost zone of the cortex, secrete aldosterone, the strongest mineralocorticoid; and those in zF, the middle zone, produce glucocorticoids such as corticosterone in most rodents and cortisol in other mammals including human. Finally, the cells in the zona reticularis, the innermost portion of the cortex, also secrete glucocorticoids in many mammals including rats and mice and produce adrenal androgens in human and some other mammals. In addition to these three, a zone composed of 3–4 layers of small round cells has been recognized between zG and zF in various animals (2–9). By using rats we showed that the cells of the zone were devoid of the two enzymes (10) determining the distinct steroidogenic functions of zG and zFR, *i.e.* aldosterone synthase (Cyp11b-2) and steroid 11β-hydroxylase (Cyp11b-1) responsible for the synthesis of corticosterone/cortisol, respectively (11). The zone thus has been named the undifferentiated cell zone (zU) (12) after the functionally undifferentiated nature of its component cells (13–18).

Development and maintenance of the adrenocortical zones require many cellular processes including regulation of the steroidogenic gene expression and regulation of cell renewal and arrangements. Steroidogenic factor 1 (19) (SF-1, also referred to as Ad4BP (20)) is a transcription factor essential for embryonic development of steroidogenic organs including adrenal cortex and gonads (21). SF-1 also plays a pivotal role in the earlier steps of the adrenocortical steroidogenesis over the entire adrenal cortex by controlling expression of cholesterol side-chain cleavage enzyme (Cyp11a) and steroid 21-hydroxylase (22). Based on these features, SF-1 is unlikely to be a key regulator for the zonal differentiation of the steroidogenesis. Regarding factors regulating expression of the steroidogenic genes for the last steps of the syntheses, we previously suggested that AP-1 transcription factors were necessary for the spatially restricted expression of Cyp11b-1 in zFR (23, 24). Other regulatory factors playing a crucial role in the zone-specific steroidogenesis of zFR have been unknown. Further-

* This work was supported in part by a grant-in-aid for scientific research from the Japan Society for the Promotion of Science, by a national grant-in-aid for the Establishment of High-Tech Research Center in a Private University, and by grants from the Mitsubishi Foundation, the Uehara Memorial Foundation, the Ichiro Kanehara Foundation, and Keio University. The costs of publication of this article were defrayed in part by the payment of page charges. This article must therefore be hereby marked "*advertisement*" in accordance with 18 U.S.C. Section 1734 solely to indicate this fact.

The nucleotide sequence(s) reported in this paper has been submitted to the DDBJ/GenBank™/EBI Data Bank with accession number(s) AB050626.

§ To whom correspondence should be addressed: Dept. of Biochemistry and Integrative Medical Biology, School of Medicine, Keio University, 35 Shinanomachi, Shinjuku-ku, Tokyo 160-8582, Japan. Tel.: 81-3-5363-3752; Fax: 81-3-3358-8138; E-mail: mukaik@sc.itc.keio.ac.jp.

¶ Present address: Dept. of Biological Science and Technology, Faculty of Engineering, the University of Tokushima, 2-1 Minamijosanjima-cho, Tokushima 770-8506, Japan.

** Present address: Dept. of Biochemistry, the University of Texas Health Science Center, San Antonio, TX 78229-3900.

[1] The abbreviations used are: zG, the zona glomerulosa; AZ-1, adrenocortical zonation factor 1; AZ-1F, FLAG-tagged AZ-1; Cyp11a, cholesterol side-chain cleavage enzyme; Cyp11b-1, steroid 11β-hydroxylase; Cyp11b-2, aldosterone synthase; DIG, digoxigenin; EGF, epidermal growth factor; GAPDH, glyceraldehyde-3-phosphate dehydrogenase; TIN-ag, tubulointerstitial nephritis antigen; TIN-ag-RP, TIN-ag-related protein; SF-1, steroidogenic factor 1; zF, the zona fasciculata; zFR, the zonae fasciculata-reticularis; zU, the undifferentiated cell zone; TBS, Tris-buffered saline.

more, no regulatory factor for the functional differentiation of the rest of the cortex, zG and zU, has been identified so far. Therefore, molecular mechanisms underlying the zonal differentiation of the adrenocortical steroidogenesis remain to be solved.

The goal of this study was to explore unidentified factors that control the functional differentiation of adrenocortical cells. To this end, we used the mouse adrenocortical cell lines that we established recently (25). They are derived from the adrenal glands of transgenic mice (26, 27) carrying a temperature-sensitive large T-antigen gene of simian virus 40, being at different degrees of differentiation from one another. In the present study, a subtractive cDNA cloning employing the adrenocortical cell lines, named AcA101 and AcA201, as well as a conventional cell line Y-1, was carried out. Among the cell lines, AcA101 is the most undifferentiated one which expresses neither Cyp11b-1 nor Cyp11b-2, whereas Y-1 is the most differentiated one that expresses Cyp11b-1 with a responsiveness to ACTH stimuli (28). A cDNA cloned from AcA101 cells by a subtractive hybridization encodes a protein termed adrenocortical zonation factor-1 (AZ-1), the subject of this paper. AZ-1 is a unique secretory protein with a preprocathepsin B-related structure carrying epidermal growth hormone (EGF) motifs. This study demonstrates that expression of AZ-1 in adrenocortical cells is inversely correlated with expression of Cyp11b-1 *in vitro* and *in vivo*.

EXPERIMENTAL PROCEDURES

Cell Culture—Mouse adrenocortical AcA101 and AcA201 cells were cultured at 33 °C, a permissive temperature for the mutant SV40 T-antigen protein, under the conditions described previously (25). Mouse adrenocortical Y-1 cells (28) were cultured at 37 °C with Ham's F-10 medium supplemented with 10% heat-inactivated fetal bovine serum (Hyclone, Logan, UT), 10% heat-inactivated horse serum (Invitrogen), 200 units/ml penicillin, and 200 μg/ml streptomycin. The cells were incubated under a humidified atmosphere containing 5% CO_2.

Subtractive cDNA Cloning—Total RNA was extracted from AcA101, AcA201, and Y-1 cells with a modified single-step isolation method employing Trizol reagent (Invitrogen). Poly(A)$^+$ RNA was prepared with an oligo(dT)-cellulose column (Amersham Biosciences) and treated with RNase-free DNase (Promega, Madison, WI). Poly(A)$^+$ RNA (2 μg) from AcA101 cells was converted into cDNA with a *Not*I-oligo(dT) primer. A cDNA library of AcA101 cells was prepared using the λZipLox system (Invitrogen) according to the instructions from the manufacturer. Subtractive probes were prepared with the chemical cross-linking subtraction method using an RNA subtraction kit (Amersham Biosciences). Single-stranded cDNA (0.4 μg) of AcA101 cells was subtracted with poly(A)$^+$ RNA (10 μg) of AcA201 or Y-1 cells by hybridization and chemical cross-linking reaction. To reduce signals from SV40 T-antigen mRNA, RNA encoding T-antigen was synthesized *in vitro* by using cloned T-antigen genes (25) and was added to the hybridization reaction. The resulting subtracted cDNA was labeled with [α-^{32}P]dCTP (3000 Ci/mmol, Amersham Biosciences) using Sequenase version 2.0 (Amersham Biosciences). The AcA101 cDNA library (2×10^5 plaque-forming units) was screened with the subtractive probes under stringent conditions. Positive plaques were isolated through a second screening process using digoxigenin-labeled cDNA (Roche Diagnostics) probes (not subtracted) from AcA101, AcA201, and Y-1 cells. Plasmids carrying a cDNA insert were recovered from λ phage clones utilizing the cre-lox systems. DNA sequencing was performed by the dideoxy termination method using Thermo Sequenase™ (Amersham Biosciences).

Northern Blotting—Total RNA was prepared from adrenal glands, whole brains, hearts, kidneys, livers, skeletal muscles, spleens, and testes of C57BL/6 mice using Trizol reagent as described above. The RNA preparations (10 μg) were subjected to Northern blot analysis as described previously (24). Before transfer to positively charged nylon membranes (Roche Diagnostics), ribosomal RNAs were visualized by ethidium bromide to verify that the amounts of RNA loaded were comparable with each other (<15%) and that degradation of the RNA preparations was undetectable under our experimental conditions. A cDNA fragment (position 1490–1810 of Fig. 1*A*) was labeled with [α-^{32}P]dCTP (3000 Ci/mmol, Amersham Biosciences) and High Prime (Roche Diagnostics). Hybridization signals were detected with a Kodak BioMax film with an intensifying screen.

Southern Blotting—Genomic DNA was prepared from the liver of CL57BL/6 mice and was digested with *Eco*RI, *Bam*HI, and *Hin*dIII. The digests (10 μg) were subjected to electrophoresis through 0.8% agarose and blotted on a positive charged nylon filter (Roche Diagnostics). A cDNA fragment of AZ-1 (position 1490–1810) was isolated and labeled with DIG-dUTP (Roche Diagnostics). Hybridization, stringent washing, and detection with color development were carried out according to the manufacturer's instructions (Roche Diagnostics) and as described previously (29, 30).

In Vitro Transcription-Translation—To construct a plasmid for expression of recombinant proteins, oligonucleotide primers for PCR were prepared. A forward primer including the putative translational initiation codon was designed to contain an artificial *Bst*XI site at position 48 of the sequence shown in Fig. 1*A*: 5′-CGCCAGTGTGCTGGAGGCACCATGTGGGGATGT-3′. A reverse PCR primer corresponding to the C terminus of the protein was designed to contain the sequence encoding FLAG epitope followed by an *Xba*I site: 5′-GCTCTAGACTACTTGTCATCGTCGTCCTTGTAGTCGTGGTGCCCCATGTCCTCC-3′. Another reverse PCR primer 5′-GCTCTAGATCAGTGGTGCCCCATGTCCTCC-3′ lacking the FLAG tag sequence was also designed. cDNA fragments (either the presence or absence of the FLAG sequence) that were amplified by PCR were inserted into pRc/CMV (Invitrogen). To avoid incorrect nucleotides incorporated in PCR, the *Dra*III fragment (position 69–1280 of Fig. 1*A*) carrying the PCR-amplified region was replaced by the authentic fragment prepared from the original cDNA. The resulting pR/C11.13FD1 and pR/C11.13D1 plasmids were used for templates in *in vitro* transcription-translation reaction of T7 TNT-coupled Reticulocyte Lysate System (Promega) in the presence or absence of [^{35}S]methionine (1000 Ci/mmol, Amersham Biosciences). Reaction mixtures were subjected to SDS-PAGE. Detection was carried out by autoradiography or immunoblotting using anti-FLAG M2 monoclonal antibody (Sigma) as described below.

Antibody Preparation—Peptides P1 (NH_2-Cys-Ser-Gln-Gly-Arg-Pro-Glu-Gln-Tyr-Arg-Arg-His-Gly-Thr-COOH) and P2 (NH_2-Cys-Gly-Arg-Val-Gly-Met-Glu-Asp-Met-Gly-His-His-COOH), corresponding to amino acid residues 386–398 and 456–466, respectively, were synthesized and each conjugated at the additional Cys residue to keyhole limpet hemocyanin (Pierce) through a thioether bond using maleimide-activated keyhole limpet hemocyanin (Pierce) as described in the instruction manual. The peptide-keyhole limpet hemocyanin conjugates were mixed (1:1 (w/w)) and emulsified with Freund's complete adjuvant and injected into IsaBrown hens 6 times intradermally at 2-week intervals. Blood was collected on the 35th day or thereafter. Antibodies were purified from antisera (10 ml) with a peptide-conjugated agarose gel column. The agarose gel was prepared by coupling a 1:1 (w/w) mixture of the two peptides using a SulfoLink coupling gel (Pierce) according to the instructions. Based on titration by an immunoblot analysis using a recombinant AZ-1 protein, the recovery of the purified antibody after the chromatography was ~70%.

In Situ Hybridization—The *Eco*RI-*Bam*HI fragment (position 1490–1810 of Fig. 1*A*) of the isolated cDNA clone was subcloned into pZL1 (Invitrogen). Mouse cDNAs encoding Cyp11b-1 (position 761–950) or Cyp11b-2 (761–953) (31) were obtained by PCR with primer pairs as described previously (25) from the total RNA of Y-1 cells after reverse transcription, and they were cloned into pGEM4-Z (Promega). DIG-labeled antisense and sense RNA probes were synthesized with T7 and SP6 RNA polymerases, respectively, using DIG RNA labeling kit (Roche Diagnostics). Mouse adrenals were excised after transcardial perfusion with phosphate-buffered saline(−) containing 4% paraformaldehyde and were further fixed with the same fixative overnight at 4 °C. The adrenals were embedded with paraffin, and 4-μm sections were prepared using 3-aminopropyltriethoxysilane-coated glass slides. After deparaffinization with standard methods, *in situ* hybridization was carried out as described previously (17). Concentrations of the antisense and sense probes (400 ng/ml) in the hybridization solutions were adjusted based on analysis by the agarose gel electrophoresis of the synthesized RNA.

Immunohistochemistry—Paraffin sections of paraformaldehyde-fixed mouse adrenal glands were treated with affinity-purified chicken anti-AZ-1 antibody (10 μg/ml) or control chicken IgY (10 μg/ml, Sigma) overnight at 4 °C. The concentrations of the antibodies were adjusted after protein determination with Coomassie Brilliant Blue G-250. The secondary antibody used was rabbit anti-chicken IgY antibody conjugated with horseradish peroxidase (1:300; Promega). The peroxidase activity was visualized with 3,3′-diaminobenzidine tetrahydrochloride and hydrogen peroxide as described previously (32).

Transfection—pR/C11.13FD1, which was the same DNA construct as

A

```
CGAGCTTGGAGGCGGAGGCGCGCAGGGCAGCCTGGGTCCAGCCCACACCCCTCACCAGGA      60

GGCACCATGTGGGGATGTTGGCTGGGGCTGCTCTTGCTGCTGCTGGCTGGCCAGGCTGCC     120
      M  W  G  C  W  L  G  L  L  L  L  L  L  A  G  Q  A▼A        18

CTGGAGGCCCGGCGGAGTCGTTGGCGCAGGGAGCTGGCGCCAGGGCTGCACCTGCGGGGC     180
L  E  A  R  R  S  R  W  R  R  E  L  A  P  G  L  H  L  R  G      38

ATCCGGGACGCCGGTGGCAGATACTGCCAAGAGCAGGACATGTGCTGTCGAGGCCGTGCT     240
I  R  D  A  G  G  R  Y  C  Q  E  Q  D  M  C  C  R  G  R  A      58

GACGAGTGTGCCCTGCCCTACCTGGGAGCCACCTGTTACTGTGACCTCTTCTGCAACCGC     300
D  E  C  A  L  P  Y  L  G  A  T  C  Y  C  D  L  F  C  N  R      78

ACCGTCTCTGACTGCTGCCCCGACTTCTGGGACTTCTGCCTCGGGATTCCACCCCCCTTC     360
I  V  S  D  C  C  P  D  F  W  D  F  C  L  G  I  P  P  P  F      98

CCTCCCGTCCAAGGGTGCATGCATGGGGGCCGGATCTACCCAGTCTTCGGAACCTACTGG     420
P  P  V  Q  G  C  M  H  G  G  R  I  Y  P  V  F  G  T  Y  W     118

GACAACTGCAATCGATGCACCTGCCATGAGGGAGGGCATTGGGAGTGCGACCAGGAGCCG     480
D  N  C  N  R  C  T  C  H  E  G  G  H  W  E  C  D  Q  E  P     138

TGTCTAGTGGACCCAGACATGATTAAAGCCATCAACCGAGGCAACTACGGGTGGCAGGCT     540
C  L  V  D  P  D  M  I  K  A  I  N  R  G  N  Y  G  W  Q  A     158

GGGAACCACAGTGCCTTCTGGGGCATGACCCTGGATGAGGGCATTCGCTACCGCCTGGGC     600
G  N  H  S  A  F  W  G  M  T  L  D  E  G  I  R  Y  R  L  G     178

ACAATCCGCCCATCCTCCACTGTCATGAATATGAATGAGATTTATACGGTGCTGGGCCAA     660
T  I  R  P  S  S  T  V  M  N  M  N  E  I  Y  T  V  L  G  Q     198

GGGGAAGTGCTACCCACTGCCTTTGAAGCTTCAGAGAAGTGGCCCAACCTGATCCACGAG     720
G  E  V  L  P  T  A  F  E  A  S  E  K  W  P  N  L  I  H  E     218

CCATTGGACCAGGGCAATTGTGCAGGTTCCTGGGCTTTCTCCACAGCAGCTGTCGCATCT     780
P  L  D  Q  G  N  C  A  G  Ⓢ  W  A  F  S  T  A  A  V  A  S     238

GATCGCGTCTCTATCCATTCTTTGGGACACATGACACCCATCCTATCACCGCAAAACCTG     840
D  R  V  S  I  H  S  L  G  H  M  T  P  I  L  S  P  Q  N  L     258

CTGTCCTGTGATACCCACCACCAGCAGGGCTGCCGAGGTGGGCGTCTTGATGGCGCTTGG     900
L  S  C  D  T  H  H  Q  Q  G  C  R  G  G  R  L  D  G  A  W     278

TGGTTCCTGCGGCGCCGCGGGGTGGTGTCTGACAACTGTTACCCATTCTCCGGCCGTGAG     960
W  F  L  R  R  R  G  V  V  S  D  N  C  Y  P  F  S  G  R  E     298

CAGAACGAGGCCAGCCCCACTCCTCGTTGTATGATGCACAGCCGCGCCATGGGGCGGGGC    1020
Q  N  E  A  S  P  T  P  R  C  M  M  H  S  R  A  M  G  R  G     318

AAGCGCCAAGCCACTTCCCGCTGCCCCAATGGTCAGGTTGATTCCAACGACATCTACCAG    1080
K  R  Q  A  T  S  R  C  P  N  G  Q  V  D  S  N  D  I  Y  Q     338

GTCACGCCTGCCTACCGCCTGGGCTCTGATGAGAAGGAGATCATGAAGGAGCTAATGGAA    1140
V  T  P  A  Y  R  L  G  S  D  E  K  E  I  M  K  E  L  M  E     358

AACGGCCCTGTTCAAGCACTCATGGAAGTACACGAGGACTTCTTCTTGTACCAGCGTGGC    1200
N  G  P  V  Q  A  L  M  E  V  H  E  D  F  F  L  Y  Q  R  G     378

ATCTACAGCCACACACCTGTAAGCCAGGGGAGGCCGGAGCAGTACCGCAGACATGGGACT    1260
I  Y  S  H  T  P  V  S  Q  G  R  P  E  Q  Y  R  R  H  G  T     398

CACTCAGTCAAGATCACTGGGTGGGGAGAAGAGACGCTGCCAGACGGAAGGACCATTAAG    1320
(H) S  V  K  I  T  G  W  G  E  E  T  L  P  D  G  R  T  I  K     418

TACTGGACTGCTGCCAACTCGTGGGGCCCATGGTGGGGTGAAAGGGGCCACTTCCGGATC    1380
Y  W  T  A  A  (N) S  W  G  P  W  W  G  E  R  G  H  F  R  I     438

GTGCGTGGCACCAACGAGTGCGACATCGAGACCTTCGTGCTGGGCGTCTGGGGTCGCGTG    1440
V  R  G  T  N  E  C  D  I  E  T  F  V  L  G  V  W  G  R  V     458

GGAATGGAGGACATGGGGCACCACTGAGTCTCAGCCACTAGGCGAGGTGGGATCCACAGC    1500
G  M  E  D  M  G  H  H  .                                      466

CACAGAAGAGGCCTTGGGGGCCATGCCCGATGAAGCCTTGTGTGCACTTCGGGACCAGGT    1560
GCTAATCTCTACAGACTCAGATCCGCGCGTGCGCGCTAAGGCAGAATCCCACCTAGGAGA    1620
CAAAGATGCACCAGGCTGGCGGAAGCCCCCAGATATCACAGCCGGAACTGGGAAGGGCCC    1680
TGTTTGGAAACTGCAGGGAGTATAGACAGATTCCAGGTCCCTGGTCAGCCAGGCCAAGAC    1740
CACAGGAGCTAAGACACCCCAACCTCATCACCCTCCTACCCACCCTCTCTCTCATCTTCT    1800
TTTTGATGAATTCTGTCCATCTCCCTAGCCTCCATTTTGGTTGTACCTTTCCATTCTCAG    1860
TACTGCTTTCTTATTCTTTAAAGATATTTATTTTTCTTTTCATTAAAATAAAACCAAAGT    1920
ATTGATAAAAAAAAAAAA                                             1938
```

B

```
                ** * *******      ** *   * ************************ *******
mouse   MWGCWLGLLLLLLAG-QAALEARRSRWRRELAPGLHLRGIRDAGGRYCQEQDMCCRGRAD  59
human   MWRCPLGLLLLLPLAGHLALGAQQGRGRRELAPGLHLRGIRDAGGRYCQEQDLCCRGRAD  60

                 ******** ************************ ****** ************ *****
mouse   ECALPYLGATCYCDLFCNRTVSDCCPDFWDFCLGIPPPFPPVQGCMHGGRIYPVFGTYWD 119
human   DCALPYLGAICYCDLFCNRTVSDCCPDFWDFCLGVPPPFPPIQGCMHGGRIYPVLGTYWD 120

                ******* *   * ***************** ****************************
mouse   NCNRCTCHEGGHWECDQEPCLVDPDMIKAINRGNYGWQAGNHSAFWGMTLDEGIRYRLGT 179
human   NCNRCTCQENRQWQCDQEPCLVDPDMIKAINQGNYGWQAGNHSAFWGMTLDEGIRYRLGT 180

                ***** **** ******  ****************************************
mouse   IRPSSTVMNMNEIYTVLGQGEVLPTAFEASEKWPNLIHEPLDQGNCAGSWAFSTAAVASD 239
human   IRPSSSVMNMHEIYTVLNPGEVLPTAFEASEKWPNLIHEPLDQGNCAGSWAFSTAAVASD 240

                ************ ************ ************************ ********
mouse   RVSIHSLGHMTPILSPQNLLSCDTHHQQGCRGGRLDGAWWFLRRRGVVSDNCYPFSGREQ 299
human   RVSIHSLGHMTPVLSPQNLLSCDTHQQQGCRGGRLDGAWWFLRRRGVVSDHCYPFSGRER 240

                 ** * * ***************  ***  *  ******** *****  **********
mouse   NEASPTPRCMMHSRAMGRGKRQATSRCPNGQVDSNDIYQVTPAYRLGSDEKEIMKELMEN 359
human   DEAGPAPPCMMHSRAMGRGKRQATAHCPNSYVNNNDIYQVTPVYRLGSNDKEIMKELMEN 360

                ****************  ********* **** ************************ **
mouse   GPVQALMEVHEDFFLYQRGIYSHTPVSQGRPEQYRRHGTHSVKITGWGEETLPDGRTIKY 419
human   GPVQALMEVHEDFFLYKGGIYSHTPVSLGRPERYRRHGTHSVKITGWGEETLPDGRTLKY 420

                ********* ************ ****** *****************
mouse   WTAANSWGPWWGERGHFRIVRGTNECDIETFVLGVWGRVGMEDMGHH              466
human   WTAANSWGPAWGERGHFRIVRGVNECDIESFVLGVWGRVGMEDMGHH              467
```

FIG. 1. **Nucleotide sequence of AZ-1 cDNA and the predicted amino acid sequence.** *A*, the amino acid sequence is shown in single-letter code *below* the nucleotide sequence. The putative cleavage site of the signal peptide is indicated by a *triangle*. The residues corresponding to those comprising the active site conserved in cysteine proteinases are *circled*. (Ser-228 in AZ-1 replaces the cysteine residue, and His-399 and Asn-424 are conserved). Two possible *N*-glycosylation sites are *underlined*. A polyadenylation signal at nucleotide position 1907–1912 is in *italics*. *B*, comparison of the amino acid sequence of *mouse* AZ-1 with that of *human* TIN-ag-RP (accession number AF236150). Identical amino acids (89%) are indicated with *asterisk*.

used for *in vitro* synthesis of FLAG-tagged AZ-1 (AZ-1F), or a control vector pRc/CMV was linearized by digestion with *Bgl*II. Y-1 cells (3×10^6) were transfected with the linearized DNA (10 μg) by calcium phosphate precipitation method using the Profection kit (Promega). The cells were selected for resistance to antibiotics G418 (400 μg/ml), and colonies were isolated and expanded for characterization as described below.

Immunoprecipitation and Immunoblotting—A mock transfectant (clone 9) and an AZ-1F vector-transfectant (clone 14; see Fig. 7), which showed the highest level of AZ-1F mRNA, were used for detection of the AZ-1 polypeptide. Cell extracts from them (3.6-cm^2 well) were prepared with an SDS sample buffer (120 μl) consisting of 62 mM Tris-HCl, pH 6.8, 2% (w/v) SDS, 2% (v/v) 2-mercaptoethanol, and 0.01% bromphenol blue. The extracts were incubated at 100 °C for 5 min before electrophoresis. For immunoprecipitation, purified chicken anti-AZ-1 antibody (150 μl) was bound to anti-chicken IgY-agarose (150 μl of 50% suspension; Promega) by incubation for 1 h at 4 °C with gentle shaking. The beads were washed with 1 ml of Tris-buffered saline (TBS) 5 times. The supernatants of the used culture media (1 ml) were prepared by centrifugation to remove cells and cell debris and incubated with 30 μl of the gel suspension for 18 h at 4 °C with gentle shaking. The agarose gel beads were washed with TBS containing 0.1% Tween 20 (TBST) 4 times followed by a wash with TBS. They were resuspended in an SDS sample buffer and treated at 100 °C for 5 min. The immunoprecipitates and the cell extracts were subjected to 10% PAGE in the presence of SDS, and polypeptides were electrophoretically blotted onto Immobilon-P membranes (Millipore, Bedford, MA) according to standard procedures. The membranes were treated with anti-FLAG monoclonal M2 antibody (0.88 μg/ml) overnight at 4 °C. They were washed with TBST and then incubated with a secondary antibody solution of rabbit anti-mouse IgG conjugated with horseradish peroxidase (1:25,000 dilution with TBST) for 3 h at room temperature. When the affinity-purified chicken anti-AZ-1 antibody (1:200 dilution) was used for immunoblotting, membranes were treated with rabbit anti-chicken IgY conjugated with horseradish peroxidase (1:1000 dilution). Bound secondary antibodies were detected by enhanced chemiluminescence (Amersham Biosciences).

Post-translational Modification—An AZ-1F-vector transfectant (clone 14) was cultured in the presence of 10 μg/ml tunicamycin (Sigma) or vehicle (0.2% (v/v) methanol in the culture medium) for 18 h, and cell extracts were prepared as described above. For treatment with peptide *N*-glycosidase F, cell extracts of the transfectant containing 2% SDS were diluted by 10-fold with 10 mM Tris-HCl, pH 7.5, and incubated with 50 units/ml of *N*-glycosidase F (Roche Diagnostics) at 37 °C for 18 h. After the treatment, the SDS sample buffer was added to the reaction mixtures. These samples were analyzed by immunoblotting as described above.

RT-PCR—RT-PCR analysis was performed by the methods as described in the previous paper (25) using primer pairs as follows: (i) AZ-1F: 64f, 5′-ACCATGTGGGGATGTTGGCTGG-3′ (position 64–85,

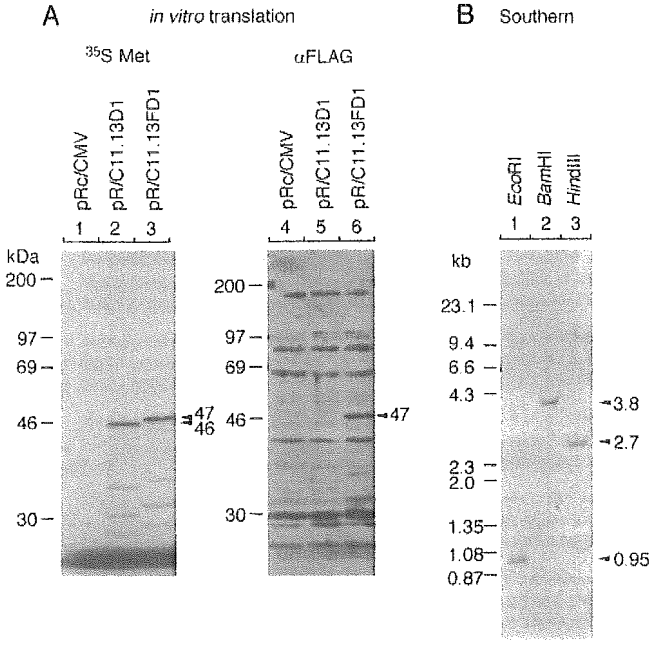

FIG. 2. ***In vitro* translation of AZ-1 polypeptide and Southern blot analysis.** *A*, *in vitro* coupled transcription-translation reaction was performed using a control vector pRc/CMV (*lanes 1* and *4*), pR/C11.13D1 (*lanes 2* and *5*), and pR/C11.13FD1 (*lanes 3* and *6*). pR/C11.13D1 and pR/C11.13FD1 carry AZ-1 cDNA and FLAG epitope-tagged AZ-1 cDNA, respectively. *Lanes 1–3*, translated products (5 μl/lane) synthesized in the presence of [^{35}S]methionine were separated on a 10% polyacrylamide gel containing 0.1% SDS and detected by autoradiography. *Lanes 4–6*, products (5 μl/lane) synthesized with non-radioactive amino acids were detected by immunoblotting using anti-FLAG antibody, a secondary antibody conjugated with horseradish peroxidase, and reagents for enhanced chemiluminescence. *B*, mouse genomic DNA was digested with restriction enzymes (*Eco*RI (*lane 1*), *Bam*HI (*lane 2*), and *Hin*dIII (*lane 3*)). The digests (10 μg/lane) were subjected to electrophoresis through 0.8% agarose gels and blotted onto a positively charged nylon filter. An AZ-1 cDNA fragment (position 1490–1810) was labeled using DIG-dUTP. Hybridization, stringent washing, and detection with color development were carried out as described under "Experimental Procedures."

see Fig. 1*A*) and FL1485r, 5′-GTCATCGTCGTCCTTGTAGTCG-3′ that corresponds to the FLAG peptide encoding sequence); (ii) AZ-1: 420f, 5′-GGACAACTGCAATCGATGCACC-3′ (420–441); 1003r, 5′-GGCT-GTGCATCATACAACGAGG-3′ (1003–982); this primer pair was used for detection of mRNA of both endogenous *Az-1* gene and AZ-1F; (iii) Cyp11b-1 (25); (iv) Cyp11a (25); and (v) glyceraldehyde-3-phosphate dehydrogenase (GAPDH) (25). Amplification conditions for PCR were 45 s at 94 °C, 45 s at 56 °C, and 2 min at 72 °C for appropriate cycle numbers followed by 7 min at 72 °C. Cycle numbers were 20 for AZ-1 (420f and 1003r), Cyp11a, and GAPDH and 25 for AZ-1F (64f and FL1485r), and Cyp11b-1. Experiments for comparison of relative amounts of mRNAs among the transfectants were performed within the exponential phase of the amplification reactions to obtain the linear response concerning the initial mRNA amounts. PCR products were analyzed by agarose gel electrophoresis followed by visualization with ethidium bromide. Intensities of the visualized products were determined by densitometric analysis and were normalized with that of GAPDH cDNA.

RESULTS

Cloning and Characterization of AZ-1 cDNA—For the subtractive cDNA cloning to identify genes whose transcripts are expressed in higher levels in undifferentiated adrenocortical cells than in differentiated cells, we prepared two probes as described under "Experimental Procedures"; one was obtained by a subtraction between AcA101 and AcA201 and the other was between AcA101 and Y-1. A cDNA library of AcA101 cells was prepared to represent the whole population of mRNA molecules. It was screened by hybridization of the two subtracted probes onto plaque lifts. We isolated cDNA clones whose hybridization signal was detected with both subtractive probes.

Among the cDNA clones isolated, one was composed of 1926 nucleotides except for a poly(A) tail as shown in Fig. 1*A*. The cDNA attracted our attention because the amino acid sequence of its encoded protein had a unique structure as described below. The protein was termed as AZ-1 since its expression level was inversely related to the degree of the functional differentiation of adrenocortical cells as described below. The cDNA contained an open reading frame encoding a polypeptide chain consisting of 466 amino acids, which was from a translational initiation codon at position 67 to a termination codon at position 1465. Several nucleotides preceding the methionine codon were consistent with the consensus sequence for translational initiation (33). A typical polyadenylation signal was found at position 1907. The N-terminal 17-amino acid sequence was predictable as a signal peptide for the secretory pathway (34). No hydrophobic region large enough to span a membrane was recognized. Possible *N*-glycosylation sites were present at Asn-77 and Asn-160. These features in the predicted amino acid sequence suggest that AZ-1 is a secretory protein.

When searched in the GenBank™/EMBL/DDBJ data base, the predicted amino acid sequence of the open reading frame had an identity of 89% with human tubulointerstitial nephritis antigen-related protein (TIN-ag-RP) (35) (Fig. 1*B*), indicating that the identified cDNA encodes a mouse orthologue of the human protein. As Wex *et al.* (35) discussed the features of amino acid sequence of TIN-ag-RP, the N-terminal one-third of AZ-1 polypeptide was rich in Cys residues and contained EGF-like repeats. The C-terminal two-thirds of AZ-1 polypeptide contained procathepsin B-related sequence with a Ser residue at position 228, which replaced a conserved Cys residue in the active site of cysteine proteinases (Fig. 1*A*), suggesting that AZ-1 does not have a proteinase activity. These structural features were also found in tubulointerstitial nephritis antigen (TIN-ag) (36–38) in mammals and also in non-mammalian homologues including *Caenorhabditis elegans* F26E4.3 protein (39).

To verify the size of the polypeptide encoded by the isolated cDNA, we carried out *in vitro* synthesis of AZ-1 using its cDNA as a template for a coupled transcription and translation reaction in the presence of [^{35}S]Met (Fig. 2*A*, *left*). As seen, the reaction with the cDNA insert (*lane 2*) gave a major product with an electrophoretic mobility of 46 kDa, which matched with the predicted molecular mass of the encoded protein. We also constructed a DNA encoding the AZ-1 polypeptide tagged with a FLAG peptide at the C terminus. The resulting FLAG-tagged polypeptide, AZ-1F, showed a band with a mobility of 47 kDa (*lane 3*). The increase of 1 kDa in molecular mass was consistent with an addition of the FLAG peptide of 8 amino acid residues to the native polypeptide. Additional bands with higher mobilities might be polypeptides where internal Met residues were used for translational initiation. The reaction with the control vector gave no signal under the experimental conditions (*lane 1*).

Transcription-translation reaction products in the absence of radioactive amino acids were examined by immunoblotting employing an anti-FLAG antibody (Fig. 2*A*, *right*). Because the control vector gave many bands under the current experimental conditions (*lane 4*), the experiment with an AZ-1-encoding template without FLAG tag resulted in no meaningful signal (*lane 5*). When the template carrying the FLAG-encoding sequence (*lane 6*) was used, the anti-FLAG antibody recognized a 47-kDa band in addition to the other bands common to *lanes 4* and *5*. Collectively, the results from *in vitro* synthesis indicated that the isolated cDNA encoded a 46-kDa polypeptide.

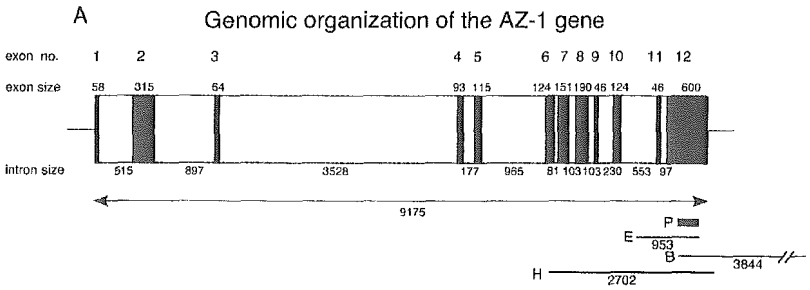

B

Exon-intron junctions in the AZ-1 gene

Exon no.	Exon size	3′-Exon junction	Intron size	5′-Exon junction	Exon no.
1	(58)	...TCACCAG^{58}gtaggg---	515	---gtctagGAGGCACCA^{67}TG.. M_1	2
2	315	...GTCCAAG^{373}gtgggc--- V Q G_{103}	897	---tggtagGGTGCAT... C M	3
3	64	...ATCGATG^{437}gtgagt--- R C_{124}	3528	---ttctagCACCTGC... T C	4
4	93	...ACTACGG^{530}gtgaga--- Y G_{155}	177	---ctccagGTGGCAG... W Q	5
5	115	...GATTTAT^{645}gtaagt--- I Y_{193}	965	---ttacagACGGTGC... T V L	6
6	124	...ACAGCAG^{769}gtgtgt--- T A A_{235}	81	---cactagCTGTCGC... V A	7
7	151	...GCCGCGG^{920}gtacgc--- R G_{285}	103	---ctctagGGTGGTG... V V	8
8	190	...CTCTGAT^{1110}gtaagt--- S D_{348}	103	---ccccagGAGAAGG... E K E	9
9	46	...GTTCAAG^{1156}gtaacc--- V Q A_{364}	230	---ccacagCACTCAT... L M	10
10	124	...TCACTGG^{1280}gtgagt--- T G_{420}	553	---cgctagGTGGGGA... W G	11
11	46	...GTACTGG^{1326}gtgagt--- Y W_{405}	97	---tcccagACTGCTG... T A A	12
12	600	...GGGCACCACTG^{1467}A...TTAAAATAAAACCAAAGTATTGAT^{1926}(A)$_n$ G H H_{466}*			

FIG. 3. **Genomic organization of the *Az-1* gene.** *A*, schematic representation of the genomic organization of the *Az-1* gene. The nucleotide sequences of the AZ-1 cDNA were located at chromosome 4 of the mouse genomic DNA sequence data base Ensembl Genome Browser (www.ensembl.org/) and span the 9175-bp sequence from position 127,681,610 to 127,672,436 in a reverse orientation. *Closed* and *open squares* represent the exons and the introns, respectively. Their sizes (bp) are shown *above* (exons) and *below* (introns) the *squares*. *Thick bar* marked with *P* represents the hybridization probe used in the Southern blot analysis of Fig. 2*B*. *Bars* marked with *E*, *B*, or *H* represent hybridization fragments predicted by restriction sites for *Eco*RI, *Bam*HI, and *Hin*dIII in the genomic sequence of the data base, being consistent with the results of the Southern analysis (Fig. 2*B*). *B*, DNA sequences of exon-intron junctions in the *Az-1* gene. *Upper* and *lowercase letters* represent the exon and the intron sequences, respectively. The encoded amino acid sequence is shown *below* the nucleotide sequence. The 5′-end of the cDNA is putatively assigned to the 5′-end of exon 1.

Southern Analysis and Genomic Organization of Az-1 Gene—Southern blot analysis was performed to ensure the presence of the *Az-1* gene in the mouse genome (Fig. 2*B*). When digested with *Eco*RI (*lane 1*), *Bam*HI (*lane 2*), or *Hin*dIII (*lane 3*), each of the digests of mouse genomic DNA gave a single hybridization signal, indicative of a single gene. Thus, the results demonstrated the presence of a genomic DNA sequence that corresponded to the isolated cDNA sequence.

To compare the AZ-1 cDNA sequence with mouse genome sequence, Ensembl Genome Browser (www.ensembl.org/) was used. The cDNA sequence was located on chromosome 4 and was encoded in 12 exons that spanned 9175 bases from positions 127,681,610 to 127,672,436 of the chromosome in a reverse direction (Fig. 3, *A* and *B*). The genomic sequences were identical to the cDNA sequence. Because the transcription start site was not determined, the 5′-end of the cDNA sequence was putatively assigned to the 5′-end of exon 1. The sizes of the hybridization signals obtained with the Southern blot analysis (Fig. 2*B*) agreed well with the restriction sites in the genomic sequence of the data base.

Distribution of AZ-1 mRNA—Expression levels of the AZ-1 mRNA in the cells used for the cloning of the AZ-1 cDNA were examined by Northern blot analysis (Fig. 4*A*). The greatest intensity of the mRNA signal (~2 kb) was observed in RNA from AcA101 cells (*lane 1*), which were used as the source of the cDNA library, among the three cell lines. A signal with a lower intensity was detected in RNA from AcA201 cells (*lane 2*), whereas no signal was obtained in RNA from Y-1 cells (*lane 3*) under the experimental conditions. Several other cell lines

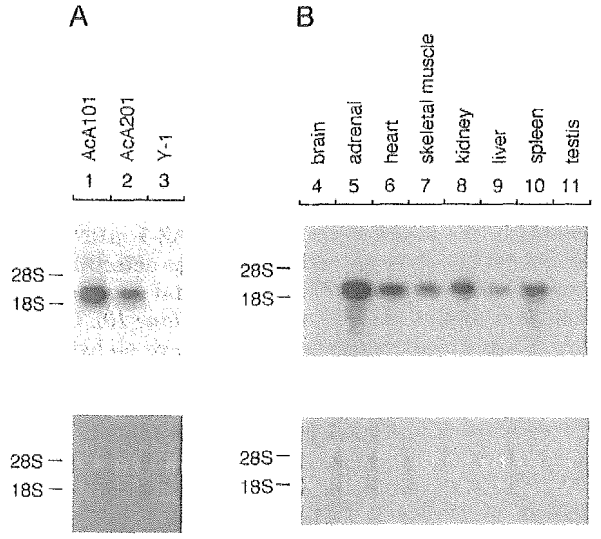

FIG. 4. **Northern blot analysis of AZ-1 mRNA.** RNA preparations (10 μg/lane) from cell lines (*A*) and from mouse tissues (*B*) were subjected to electrophoresis through 1% agarose gels and transferred onto a positively charged nylon filter. Before transfer, rRNAs (*28S* and *18S*) were visualized by ethidium bromide to verify that amounts of RNA loaded were comparable with each other and that degradation of the RNA preparations was undetectable under the experimental conditions. An AZ-1 cDNA fragment (position 1490–1810) was labeled using [α-^{32}P]dCTP. Hybridization, stringent washing, and detection by autoradiography were carried out as described under "Experimental Procedures."